Kinetics and Catalysis, Vol. 41, No. 4, 2000, pp. 462–484. Translated from Kinetika i Kataliz, Vol. 41, No. 4, 2000, pp. 511–534.

Mathematical Modeling of Kinetics of Adenosine-5'-triphosphate Hydrolysis Catalyzed by the Zn^{2+} Ion in the pH Range 8.5–9.0

E. Z. Utyanskaya*, B. V. Lidskii, M. G. Neigauz**, and A. E. Shilov***

* *Emanuel Institute of Biochemical Physics, Russian Academy of Sciences, Moscow, 117977 Russia*
** *Semenov Institute of Chemical Physics, Russian Academy of Sciences, Moscow, 117977 Russia*

Received November 23, 1998

Abstract—The kinetics of adenosine-5'-triphosphate (ATP) hydrolysis catalyzed by Zn^{2+} at pH 8.5–9.0 is analyzed by numerical simulation. The rates of product formation (adenosine diphosphate (ADP) and adenosine monophosphate (AMP)) are determined by a conformational transformation. In the sequence of steps of mutual transformations of cyclic (Cy) pH-dependent species, which are active in ATP hydrolysis to ADP, and open (Op) species, the rate-limiting step is the slow isomerization of $ZnATP^{2-}$ complexes. This slow step is determined by the abstraction of the OH^- group from a pentacovalent intermediate catalyzed by H_3O^+. In the Op species, Zn^{2+} is bound to the phosphate chain. In the Cy species, which can be hydrolized to ADP, Zn^{2+} coordinates a nitrogen atom in position 7 and γ-phosphate. The mutual transformations of conformers occur via pentacovalent intermediates with the participation of γ-phosphorus and include pseudotransformations. In the direct transformation $CyOH^- \rightleftharpoons OpOH^-$, pseudotransformation is a rate-controlling step. The deprotonated open monomeric form $OpOH^-$ is inactive in hydrolysis. Within the framework of the dimeric model and a more complex model that accounts for the role of trimeric associates $ZnATP^{2-}$, the general scheme of intermediate transformations is considered that accounts for the existence of a pH-independent pathway of hydrolysis. The rate and equilibrium constants are estimated. Concentration profiles for intermediate products during hydrolysis are described.

INTRODUCTION

Dephosphorylation of adenosine-5'-triphosphate (ATP) is one of the most important biological processes, which releases the energy of the macroergic bond. In the catalysis of phosphoryl group transfer in enzymatic and model catalytic systems, the ions of two-valent and variable-valence metals play a very important role [1–23]. The chemical mechanism of the transformation of ATP energy during its hydrolysis into other forms of energy is yet unclear. All ATP-ase systems that catalyze ATP hydrolysis to adenosine diphosphate (ADP) and inorganic phospate (P_i) and ATP synthesis are metalloenzymes and contain one or several metal ions M^{2+} in the active center. The kinetics of the hydrolysis of ATP and other polyphosphates catalyzed by many peptide enzymes is very complex. In many cases, conformational changes in enzymes are rate-determining steps of the overall process [24, 25]. In myosin-catalyzed ATP hydrolysis, a decrease in the free energy largely occurs at the stage of ATP binding to an enzyme ($\Delta G = -53$ kJ/mol). A small decrease in the free energy accompanies the reversible hydrolysis of bound ATP, which results in the formation of ADP and P_i bound to the enzyme ($\Delta G = -5.4...-11.7$ kJ/mol). Only the release of the products (ADP and P_i) from the enzyme requires some energy (ΔG = 21–25 kJ/mol). The rate-determining step of hydrolysis is the isomerization of myosin, which precedes the abstraction of products and their release to the medium [24, 25]. Kandal *et al.* [26] have shown that the addition of dimethyl sulfoxide (DMSO) is very favorable for the formation of enzyme-bound ATP from medium P_i by mitochondrial adenosinetriphosphatase that has tightly bound ADP present. Mutual transformations of bound ATP into bound ADP and P_i are much faster than the interaction of P_i with the enzyme, and the addition of DMSO favors the addition of P_i to the enzyme [26]. Therefore, ATP-ase contains functional groups that rapidly and reversibly catalyze ATP hydrolysis to form bound ATP and P_i and the groups participating in the deactivation of intermediate products of hydrolysis. This leads to conformational changes in the enzyme and product desorption. It remains unclear which functional groups of enzyme aminoacid residues catalyze ATP hydrolysis and why they are active only in the presence of the M^{2+} ions.

Recent advances in the field of model systems with metal ions are associated with the application of modern physicochemical methods of analysis. The most important findings include (i) the determination of stability constants of binary $MATP^{2-}$ complexes, as well as ternary (mixed-ligand) $MATP^{2-}$ complexes with OH^-, NH_3, aromatic nitrogen-containing heterocycles, imidazole, or other ligands, (ii) the determination of the deprotonation constants of water coordinated to an M^{2+} ion, (iii) the determination of the composition, complexation sites, and the structure of initial and some intermediate complexes by ^1H, ^{13}C, and ^{31}P NMR

0023-1584/00/4104-0462$25.00 © 2000 MAIK "Nauka/Interperiodica"

[7, 11, 15, 19, 29–32, 34, 35]; IR and Raman spectroscopy [36, 37]; and other methods. Nevertheless, many problems concerning the structures of active complexes remain open. In many kinetic studies, the initial rates of the dephosphorylation of ATP and its complexes with M^{2+} are analyzed. The data on pathways of formation and transformation of intermediates in the hydrolysis of $MATP^{2-}$ complexes are very scarce.

In 1986–1989, we proposed a structural model for the reactive center of hydrolysis. In this center, the active $M^{2+}OH^-$ anion is in the opposite position to the P_γ–OP_β bond, which is cleaved (the cyclic conformation of the $MATP^{2-}$ complex, Fig. 1a). The position of this anion is due to the coordination of M^{2+} by the N7 atom of the proper adenine base and by the O^- atom of the proper γ-phosphate group. More recently, we obtained kinetic and thermodynamic evidence for this structure of the active monomeric cycle [38–44]. The Zn^{2+} ion in the cyclic monomeric species $ZnATP^{2-}$ reacts with one O^- atom of γ-phosphate directly and with another O^- via a coordinated water molecule. Because the Zn^{2+} ion strengthens the acidic properties of a coordinated water molecule, the hydrogen bond of hydrated water with the phosphate becomes stronger than in the absence of M^{2+} [36]. When the proton is abstracted from the coordinated water molecule, the hydrogen bond between the $Zn^{2+}OH^-$ ion and the O^- of the terminal phosphate cleaves. The $Zn^{2+}OH^-$ ion holds the opposite position to the γ-P atom. Figure 1b shows the assumed structure of the monomeric open form of the $ZnATP^{2-}$ complex (Op), which is assumed to be a β,γ-conformer [37]. Open and cyclic (Cy) isomers differ in the spatial arrangement of coordinated water. The Zn^{2+} ion is bound directly to different terminal O^- atoms [44]. The inability of Op to cleave the P_γ–OP_β bond is probably due to its conformation: in Op, the coordinated H_2O molecule forms the OH^- group bound to Zn^{2+} in the plane perpendicular to the P_γ–OP_β bond, which is cleaved. Therefore, the $Zn^{2+}OH^-$ ion cannot attack the γ-P atom of ATP. The active dimeric species consists of two $ZnATP^{2-}$ molecules, each containing a cyclic triphosphate chain, and each Zn^{2+} ion is bound to the N7 atom of the proper adenine base and a proper phosphate group. In the reactive center of the dimer, the N1 atom of the adenine base of the second $ZnATP^{2-}$ molecule abstracts the proton from the coordinated water molecule, which is opposite to the γ-phosphate group. Then, this N1 transfers proton to the γ-phosphate group in a fast equilibrium step, and a hydrogen bond is formed between the γ-phosphate group bound to Zn^{2+} and the N1 atom of the second $ZnATP^{2-}$ molecule (a complex with the $(ZnATP^{2-})_2H^+OH^-$ composition, Fig. 1c) [39–41, 43]. The spatial structure of the complex enables the further interaction of coordinated OH^- with the P atom of the γ-phosphate group and the hydrolysis of the latter to form ADP and P_i. Our kinetic data on ATP hydrolysis in the Zn · ATP (1 : 1) system supports the dimeric model described above [41–44] and the role of the N1 atom of the second ATP molecule

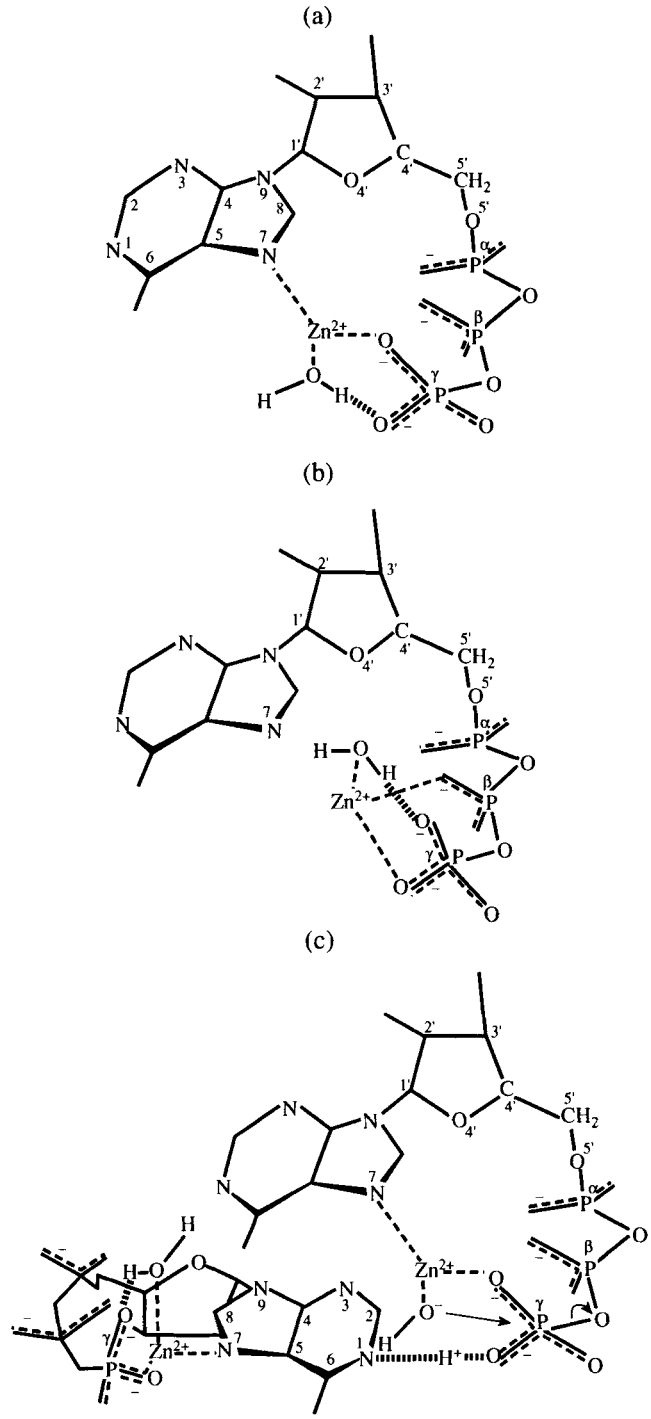

Fig. 1. Assumed structure of (a) the cyclic $ZnATP^{2-}$ species (Cy), (b) the monomeric open $ZnATP^{2-}$ species (Op), and (c) the dimeric complex (D) formed from two molecules of the monomeric cycle, an intermediate in the pH-independent hydrolysis pathway.

as a general base catalyst. The close values of rate constants of hydrolysis point to the fact that ATP conformations in these forms are analogous. The participation of nitrogen atoms from the adenine part of the second ATP molecule in the creation of the conformation which is spatially prepared to hydrolysis is analogous to the mechanism of enzyme and riboenzyme action

[2, 24, 26, 45–47]. The second $ZnATP^{2-}$ molecule acts as the simplest enzyme analog. This molecule is located near a water molecule coordinated by the M^{2+} ion and favors the equilibrium deprotonation of water and the formation of the OH^- ion in the coordination sphere of M^{2+}. We consider the solvation of the proton to form a strong hydrogen bond during the formation of intermediate complexes in hydrolysis as a factor that favors the formation of the nucleophile for an attack. Deprotonated amine or amide groups of aminoacid residues act similarly to the N1 atom in the enzymatic phosphoryl-transfer reactions. It was shown in [44] that the formation of ADP and AMP at pH > 8.5 occurs via two parallel pathways from the start of the reaction. This is in contrast to the reaction at pH 7–8.2. The fraction and rate of AMP formation increase with an increase in pH. At pH 8.5–9.1, AMP is generated via the equilibrium formation of doubly protonated open species $Op(OH^-)_2$, which in turn is formed from $CyOH^-$ and OH^-. Analysis of hydrolysis kinetics at pH 8.5–9.1 allowed us to assume that the place for the cleavage of the phosphate chain is determined by its conformation: the cyclic species (Cy_2 and $CyOH^-$) are active toward the formation of ADP and P_i, whereas the open species $Op(OH^-)_2$ is active toward the formation of AMP and pyrophosphate. The data obtained in [43, 44] motivated the consideration of the mechanism of the isomeric transformation of open (in the Op species, Zn^{2+} is bound only to the phosphate chain) and cyclic pH-dependent species, which are active in hydrolysis with the formation of ADP. In this article, we report the results of the computational modeling of the experimental hydrolysis kinetics. The goals of this modeling are (1) to confirm and develop the principle of the general base catalysis by amine in the process of ADP and P_i formation from the $(ZnATP^{2-})_2H^+OH$ dimer; (2) to elucidate the pathways for the mutual transformations of the conformer ATP complexes with the Zn^{2+} ion; (3) to develop a general scheme for intermediate product transformations over wide ranges of pH and concentrations and to estimate the rate and equilibrium constants of the intermediate steps; (4) to determine the intermediate steps of hydrolysis in which the H_3O^+ and OH^- ions of the medium participate; and (5) to elucidate active intermediates in hydrolysis, including pentacovalent phosphorus compounds using the kinetic methods. In this work, we consider hydrolysis at pH 8.5–9.0.

EXPERIMENTAL AND CALCULATION METHODS

ATP and $Zn(NO_3)_2$ solutions were prepared and kinetic experiments were carried out as described in [41, 43, 48]. To analyze the mixture of hydrolysis products, we used the method of ion-pair high-performance liquid chromatography with reversed phases on a sorbent with grafted C-18 groups. To separate ATP, ADP, and AMP in the isocratic regime under mild conditions, Separon SGX C-18 was used as a stationary phase. The conditions of analysis were as follows: room temperature, pH 6.8–6.9, and the KH_2PO_4 buffer (0.10–0.15 mol/l). An ion-couple agent was tetrabutylammonium hydroxide (3 mmol/l). The concentration of methanol in an eluent was 7–10 vol % [48]. The application of ion-couple chromatography that ensures the yield with short retention times of weak AMP and ADP peaks and a much longer retention time for the intensive ATP peak enabled us (1) to study fine effects of AMP formation under conditions when its concentration changed only slightly during hydrolysis (from 1 to 3–6 mol %), (2) to reach a high accuracy in the determination of the ADP concentration (from 1 to 5–20 mol %), and (3) to avoid complications due to the effect of Zn^{2+} ions, which are present in the reaction mixture. This made possible the quantitative description of the kinetic curves for the product formation and estimation of the rate constants of fast steps by the combined analysis of the induction period and the rates of AMP and ADP formation. All experiments were carried out at 50°C and certain values of pH, which were kept constants by adding a solution of NaOH of the known concentration. The reaction start was considered to be an instant pH attained a preset value from the side of lower pH. The samples taken were immediately diluted to reach the pH of the solution within 3.5–4.5 and the overall concentration of nucleoside phosphates within $(0.5–1.2) \times 10^{-3}$ mol/l and then frozen. Before analyses, the samples were melted and separated in a centrifuge. Then, they were injected into a chromatograph via a doser in an amount of 5–20 μl. The initial rates of ATP consumption (w_0) were measured at the initial linear portions of kinetic curves:

$$w_{0,\,ATP} = (-d\alpha_{ATP}/dt)[NuP]_0, \quad (1)$$

where $[NuP]_0 = [AMP]_0 + [ADP]_0 + [ATP]_0$; NuP is nucleoside-5'-phosphate; and α_{ATP} is the molar fraction of ATP. The initial rates of ADP formation were found from the kinetic curve of [ADP] increase

$$w_{0,\,ADP} = (d\alpha_{ADP}/dt)[NuP]_0, \quad (2)$$

where α_{ADP} is the molar fraction of ADP. The initial rates of AMP formation were measured in an analogous way. For each sample, two or three values determined in parallel measurements were averaged (these differed by at most 0.1–0.2 mol %).

The rate constants of reactions under study were determined by solving an inverse kinetic problem, which consists in finding a correct kinetic scheme of reactions and determining the numerical values of rate constants that describe the experimental kinetics for ADP and AMP formation within the sufficient accuracy at different values of pH and initial concentrations. We took into account that some values of rate and equilibrium constants were determined in the experiments [41, 43, 44]. This task was solved by the purposeful all variants by extending the kinetic scheme and making it

more complex: the initial scheme for pH ≥ 8.5 had 17 reactions and 11 species, whereas the final scheme had 67 reactions and 36 species. The kinetic experiments were divided into series depending on pH or initial concentrations. Within each series, we isolated the groups of rate constants that were critical for the reaction kinetics. We also took into account physical constraints on the region of allowable values of the rate constants.

The direct kinetic problem (kinetic simulation with a set of constants) was solved using the standard program that accommodated the procedure developed by us. The set of kinetic equations is a set of stiff nonlinear ordinary differential equations of the form

$$d\mathbf{x}/dt = \mathbf{F}(x). \quad (3)$$

Here, $\mathbf{x}(t)$ is the unknown vector of concentrations, $\mathbf{x}(0)$ is the vector of initial concentrations, and $\mathbf{u}(t) = \mathbf{x}(t) - \mathbf{x}(0)$. Set (3) can be written in the form

$$d\mathbf{u}/dt = \mathbf{A}\mathbf{u}(t) + \mathbf{b}(\mathbf{u}), \quad (4)$$

where $\mathbf{b}(\mathbf{u}) = \mathbf{F}(\mathbf{x}(0)) + \mathbf{u}(t) - \mathbf{A}\mathbf{u}(t)$; $\mathbf{A}$ is the constant matrix, which can be calculated as a matrix of linear approximation; and it is considered constant in some interval of t. Then, using a certain criterion, the matrix $\mathbf{A}$ is calculated again.

The unknown function $\mathbf{u}(t)$ is the solution to the set of nonlinear equations

$$\mathbf{u}(t) = \mathbf{C}(t)\mathbf{b}(\mathbf{u}(t)), \quad (5)$$

where $\mathbf{C}(t) = \mathbf{A}^{-1}(\exp(\mathbf{A}t) - \mathbf{E})$ and $\mathbf{E}$ is the unity matrix.

The matrix $\mathbf{C}(t)$ can be calculated with a high accuracy using the fractional–quadratic approximation for the matrix exponent. Thus, the $\mathbf{C}(t)$ matrix should not be calculated at each integration step. Rather, we can do it only sometimes and thus reduce the time for computation. Nonlinear equation (5) is solved using the Newton method modified by us. These are the main stages of solving the forward kinetic problem.

Based on the data for different pH regions, we constructed the total scheme of transformations within the framework of the dimeric model. The method described above was used to simulate all series of experiments at pH 7.1–9.0. When searching for a rate constant of each step, we tried several variants and obtained the range of rate constant values at which the experimental data are described adequately. The other parameters were kept constant. Then, inside the ranges found for each constant, we found the best value. For each new scheme of transformations, we had to modify the program because of changes in the initial conditions. The most difficulties appeared when constructing the final model that accounts for trimers. This model has many parameters and requires finding an agreement between the rate constants in different pH ranges.

RESULTS AND DISCUSSION

Table 1 shows the conditions for the experiments, the results of which were analyzed below. Figure 2 shows the kinetic curves of ATP consumption and ADP and AMP formation at pH 8.58 (run 2). These kinetic curves are typical at pH ≥ 8.5. At the initial stage, the molar fraction of ATP substantially decreases, and the molar fractions of ADP and AMP increase. When the conversion of ATP reaches 4.8–5.1%, the rates of ATP consumption and ADP and AMP formation become almost constant. In the series of experiments at $[Zn \cdot ATP]_0 = 2.72 \times 10^{-3}$ mol/l (runs 1–7), the sum of initial rates of ADP and AMP formation was equal to the initial rate of ATP consumption [43]. The same equality was observed after reaching a conversion of 4.8% [44] and in the experiments at higher concentrations (Table 2). Therefore, up to an ATP conversion of 10%, the ADP is formed in parallel with AMP from the start of the reaction (after the induction period with respect to AMP, which was small in this region of pH and changed from 8.2 min at pH 8.5 to ~2 min at pH 9, see Table 3). The presence of the induction period of AMP formation is associated with the fast and equilibrium formation of the open species $Op(OH^-)_2$ from $CyOH^-$ and OH^- [43].

Kinetic Scheme without Detailed Analyses of the pH-Independent Hydrolysis Pathway

The sequence of steps proposed in [44] for transformations of intermediates at pH 8.5–9.1 is shown in Scheme 1. This scheme assumes that $CyOH^-$ participates in the formation of ADP and $Op(OH^-)_2$, which leads to AMP and isomerizes to $OpOH^-$ via an intermediate $Cy'OH^-$. This process is characterized by the rate constant k_7. There is a fast equilibrium between $Cy'OH^-$ and $CyOH^-$. The fraction of $Cy'OH^-$ among all $CyOH^-$ species is small. The isomerizations of Op into Cy (step 5) and $OpOH^-$ into $CyOH^-$ (step 7) are slow. That is, the transformations of unreactive β,γ-complexes of $ZnATP^{2-}$ and $ZnATP^{2-}OH^-$ (Op and $OpOH^-$) into active Cy and $CyOH^-$ complexes containing Zn^{2+} coordinated to the γ-phosphate group are slow. A high reactivity of the $CyOH^-$ ion in the isomerization processes reveals itself in the formation of $Op(OH^-)_2$ during the first 1–8 minutes of the reaction. Then, the equilibrium Cy + $CyOH^-$ + $Op(OH^-)_2$ mixture transforms into the equilibrium mixture of inactive species Op + $OpOH^-$ via the intermediate formation of $Cy'OH^-$. The forward and reverse $CyOH^- \rightleftharpoons Cy'OH^-$ reactions are catalyzed by the OH^- ion. Steps 3 and 4 are fast protolytic equilibrium ionization reactions of coordinated water from the monomeric species of $ZnATP^{2-}$ (Op and Cy). Experiments at pH ≥ 8.5 showed that all kinetic curves at an ATP conversion of ≥4.8–5.0% have segments corresponding to the slower formation of ADP, AMP, and ATP consumption. At these segments, the concentrations of active

Table 1. Experimental conditions at pH ≥ 8.5

No. of run	pH	$[NuP]_0^* \times 10^3$, mol/l	$[Zn^{2+}] \times 10^3$, mol/l	$[NaClO_4]^{**}$, mol/l	$[Zn \cdot ATP]_0^{***} \times 10^3$, mol/l	$[ZnATP^{2-}]_0^{****} \times 10^3$, mol/l
1	8.50 ± 0.02	2.87	2.74	0.110	2.70	1.89
2	8.58 ± 0.02	2.85	2.73	0.112	2.73	1.72
3	8.73 ± 0.02	2.83	2.71	0.111	2.71	1.49
4	8.84 ± 0.03	2.84	2.72	0.111	2.72	1.33
5	8.96 ± 0.03	2.84	2.72	0.111	2.72	1.18
6	9.02 ± 0.04	2.84	2.72	0.109	2.72	1.07
7	9.11 ± 0.03	2.84	2.72	0.109	2.72	0.95
8	8.51 ± 0.04	5.00	4.79	0.118	4.79	3.17
9	8.75 ± 0.04	6.44	6.14	0.112	6.14	3.38

* The total initial concentration of nucleoside-5'-phosphates.

** The $NaClO_4$ concentration in a cell.

*** Zn · ATP means that Zn^{2+} is in the amount equivalent to ATP (without indicating species present).

**** The initial concentration $ZnATP^{2-}$: $[ZnATP^{2-}]_0 = a[Zn \cdot ATP]_0$, where a is the molar fraction of $ZnATP^{2-}$ in the balance of species at a given value of pH (according to the results of potentiometric titration [6]).

monomeric species $CyOH^-$, responsible for the formation of ADP via the pH-independent pathway of hydrolysis and $Op(OH^-)_2$ responsible for the formation of AMP + PP_i change insignificantly with time. The numerical values of equilibrium deprotonation constants of H_2O coordinated to Zn^{2+}, which provide a good fit to the experimental data ($K_{a,Cy} = 0.84 \times 10^{-9}$ mol/l and $K_{a,Op} = 1.64 \times 10^{-9}$ mol/l [43, 44]), point to the fact that the conformers are almost equally active in H^+ abstraction from the coordinated water molecule. The reaction of the N7 atom substitution for OH^- in the coordination sphere of Zn^{2+} (step 6) is much faster than the formation of Cy from Op in step 5 and deteriorates the equilibrium ratio $[Op]_0/[Cy]_0 \approx 2.6$ [4, 27, 28], which is settled at more acidic pH [43, 44]. At pH > 8.5, this takes place at an early stage of hydrolysis.

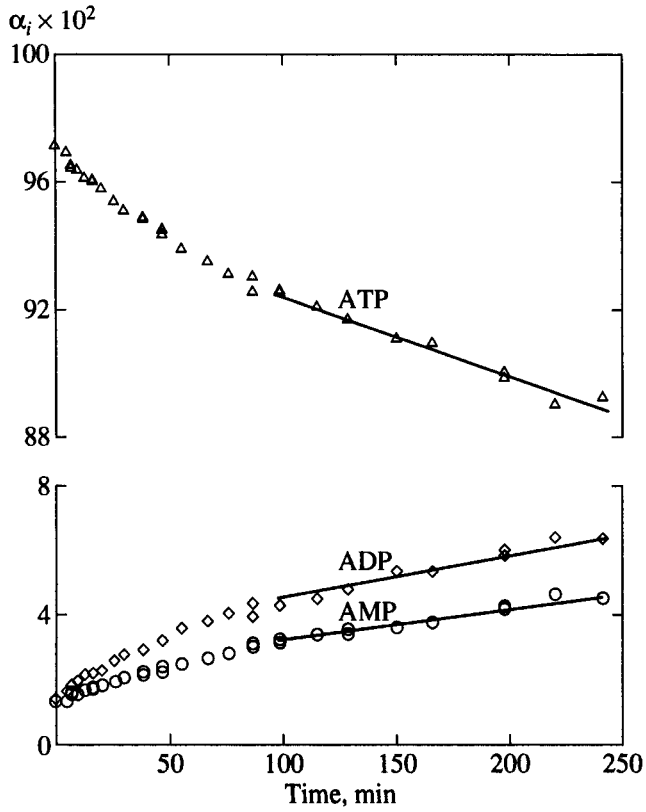

Fig. 2. Kinetic curves of ATP consumption and ADP and AMP formation at pH 8.58 ($[Zn \cdot ATP]_0 = 2.73 \times 10^{-3}$ mol/l, $[NaClO_4] = 0.112$ mol/l, and 50°C).

Table 4 shows estimated changes in the composition of the reaction mixture when the equilibrium is established in step 6 at the end of the induction period of AMP formation [44]. The estimates are based on the initial rate of ADP formation using the following values: $K_{a,Cy}$ and $k_1 = 7.6 \times 10^{-3}$ min^{-1} (the experimental rate constant of ADP formation from the monomeric $CyOH^-$ species [43], $k_2 = 1.13 \times 10^{-2}$ (the experimental rate constant of ADP formation in the pH-independent pathway of dimer hydrolysis [41]), $K'_D = 179$ l/mol (the equilibrium constant of dimer formation from two monomeric Cy molecules calculated from the k_2K_D value in the series of experiments at $[Zn \cdot ATP]_0 = (2.74 \pm 0.04) \times 10^{-3}$ mol/l [43, 44]. The initial rate of ADP formation was described by the equation [44]

$$w_{0,ADP} = k_2K'_D[Cy]^2 + k_1[CyOH^-]. \quad (6)$$

Given the initial rate, expression (6) allows us to calculate [Cy] and $[CyOH^-]$. To estimate the changes in the composition, we assumed that $[Cy]_0 + [Op]_0 = [ZnATP^{2-}]_0$ and $[Op]_0/[Cy]_0 = 2.6$ at the initial moment. The molar fraction of $ZnATP^{2-}$ among all Zn · ATP species at a given value of pH was determined by

Table 2. The initial rates of ATP consumption and ADP and AMP formation under the conditions when ADP and AMP are formed in parallel

No. of run	pH	$[Zn \cdot ATP]_0 \times 10^3$, mol/l	$w_{0,ATP} \times 10^7$, mol l^{-1} min^{-1}	$w_{0,ADP} \times 10^7$, mol l^{-1} min^{-1}	$w_{0,AMP} \times 10^7$, mol l^{-1} min^{-1}
8	8.51 ± 0.04	4.79	42.4 ± 9.9	30.0 ± 6.3	14.8 ± 5.2
9	8.75 ± 0.04	6.14	55.5 ± 6.7	35.3 ± 5.5	22.2 ± 3.7

potentiometric titration [6]. Changes in the stability constants of monomeric $MATP^{2-}$ complexes showed that the $ZnATP^{2-}$ complexes exist in the aqueous solutions in two forms (open and closed, i.e., Cy' cyclic) [1, 4, 27, 28, 31]. The equilibrium is rapidly established between these forms of the $MATP^{2-}$ complex at pH ~ 7 [28–31]. In calculations, we also used the approximate value of the equilibrium constant for the formation of the $Op(OH^-)_2$ species from $CyOH^-$ and OH^- ($K'_{eq} = 3.6 \times 10^4$ l/mol). This value was estimated from the data on the rate of AMP formation after the induction period [44]. The concentrations of different species in mol % are specified in Table 4 with reference to $[Zn \cdot ATP]_0$. It follows from Table 4 that, when the equilibrium of $Op(OH^-)_2$ formation is established, only a fraction $\Delta([Cy] + [CyOH^-])$ is consumed for the formation of $Op(OH^-)_2$. For instance, at pH 8.58, an overall decrease in the [Cy] + $[CyOH^-]$ concentration is 7.3 mol % of which only 2.9 % goes to the formation $Op(OH^-)_2$, of ADP, and AMP (0.2%), whereas 4.2% returns to the composition of the equilibrium [Op] + $[OpOH^-]$ mixture. The [Op]/[Cy] = 3.5–5.0 ratio found from the initial rates is higher than the same ratio (2.6) at an early stage of hydrolysis at pH 7.1–8.2. The values listed in Table 4 suggest that the Op ⇌ Cy equilibrium is deteriorated from the start of the reaction. This is not due to the formation of $Op(OH^-)_2$, but also to the direct transformation of $CyOH^-$ into $OpOH^-$ at pH > 8.5.

During hydrolysis, the concentrations of active Cy, $CyOH^-$, and $Op(OH^-)_2$ species decrease because of $CyOH^-$ transformation into $OpOH^-$ and Cy transformation into Op. These concentrations are settled at a low unchanging level because of the slow conversion of Op into Cy and $OpOH^-$ into $CyOH^-$. The slow formation of Cy and $CyOH^-$ plays the main role in the formation of ADP and AMP under these conditions. The scheme proposed for pH > 8.5 describes well the transformations of monomers. At the segment of the kinetic curve where the rates of ADP and AMP formation change only slightly, the [Op]/[Cy] ratio reaches 16–18 at pH > 8.8, and the corresponding $[OpOH^-]/[CyOH^-]$ ratio increases to 32–34 (Table 5). In the calculation of the values listed in Table 5, the changes in the ratios $[CyOH^-]/[Zn \cdot ATP]_0$, $[Cy]/[Zn \cdot ATP]_0$, and $[Op(OH^-)_2])/[Zn \cdot ATP]_0$ were calculated from a decrease in the rates of ADP and AMP formation with respect to the same rates at the end of the induction period for AMP. Then, we found a change in $\Delta([Op] + [OpOH^-])$ in mol % with respect to $[Zn \cdot ATP]_0$. Using the $K_{a,Op}$ value, we determined the separate concentrations of Op and $OpOH^-$ at any moment t. Table 5 shows that a noticeable part of a concentration change of the equilibrium mixture $\Delta([Cy] + [CyOH^-] + [Op(OH^-)_2])$ is not associated with the formation of final products (ADP and AMP). Rather, it is due to the transformation into the mixture of inactive species Op + $OpOH^-$. For instance, of the overall decrease in the equilibrium mixture concentration $\Delta\{[Cy] + [CyOH^-] + [Op(OH^-)_2]\}$, which is 15 mol % at pH 8.96, only 5 mol % is due to an increase in the concentrations of ADP and AMP, but 10 mol % is due to an increase in the concentration

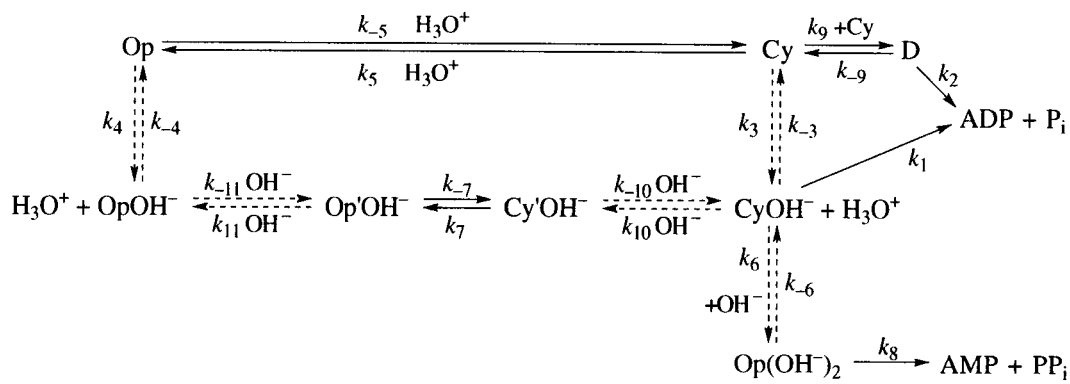

Scheme 1

Table 3. Experimental and calculated values of the induction period of AMP formation at different values of the rate constants of $Op(OH^-)_2$ formation from $CyOH^-$ and OH^- (k_6) and the reverse reaction of $Op(OH^-)_2$ decomposition (k_{-6}) (see Scheme 1)

No. of run	pH	$\tau_{ind, AMP}$, min		
		experiment	calculation according to variant 5	calculation according to variant 6
1	8.50	8.2	13–18	8.5
2	8.58	~5–6	13–16	5–8
3	8.73	~4–6	9–13	4.3
4	8.84	~3	–	4–5
5	8.96	~4	5–8	3–4
6	9.02	~2	5–8	2–3
7	9.11	~2	4–8	2–3

$\Delta([Op] + [OpOH^-])$. Therefore, there is an additional mechanism for a decrease in the Cy concentration, which is associated with the transformation of the ions $CyOH^- \rightleftharpoons OpOH^-$. This mechanism further disturbs this equilibrium and the equilibrium $Cy \rightleftharpoons Op$.

Earlier, we showed that the apparent rate constant of ADP formation from $ZnATP^{2-}$ ($k_{app} = w_0/[ZnATP^{2-}]_0$) linearly depends on $1/[H_3O^+]$ in three series of experiments with different initial $ZnATP^{2-}$ concentrations at pH 7.1–8.2 [43]. This dependence for the initial rates (w_0) of ATP consumption is fulfilled under conditions when the induction periods of AMP formation are rather long and the active monomeric species $CyOH^-$ is in equilibrium with Cy. The equilibrium between Cy and $Op(ZnATP^{2-})$ is fast and the ratio $([Op]/[Cy])_0 = b = 2.6$ does not depend on pH. The fraction of the dimer is small as compared to the monomer fraction,

Table 4. Concentrations of cyclic and open species of $ZnATP^{2-}$ and the corresponding $ZnATP^{2-}OH^-$ species after attaining the equilibrium in step $CyOH^- + OH^- \rightleftharpoons Op(OH^-)_2$ (Scheme 1)

pH	8.50	8.58	8.73	8.84	8.96	9.02	9.11
$[OH^-] \times 10^5$ mol/l	1.73	2.08	2.94	3.79	4.99	5.73	7.05
[Cy], mol %	12.6	12.1	9.9	5.6	6.8	7.3	4.8
[Op]/[Cy]	4.3	4.0	4.2	7.2	4.6	3.5	5.1
$[CyOH^-]$, mol %	3.3	3.8	4.5	3.3	5.2	6.4	5.2
$[OpOH^-]/[CyOH^-]$	8.3	8.3	8.7	13.3	8.9	7.0	9.8
$[Op(OH^-)_2]$, mol %	2.0	2.9	4.7	4.5	9.3	13.1	13.1
$\Delta^*[ADP] + \Delta[AMP]$, mol %	0.7	0.2	0.2	0.2	0.1	0.4	0.2
$\Delta^*([Cy] + [CyOH^-])$, mol %	8.7	7.3	7.8	13.1	9.1	6.2	10.2
$\Delta^*([Op] + [OpOH^-])$, mol %	6.0	4.2	2.9	8.4	0.3	7.3	3.1

* The symbol Δ denotes a change in the corresponding value after the attainment of equilibrium.

Table 5. Concentrations of cyclic and open species of $ZnATP^{2-}$ and the corresponding species $ZnATP^{2-}OH^-$ during hydrolysis in the beginning of the region where the rates of ADP and AMP formation are approximately constant

pH	8.50	8.58	8.73	8.84	8.96	9.02	9.11
[Cy], mol %	9.1	6.1	3.8	2.3	2.0	2.0	1.5
[Op]/[Cy]	6.0	8.4	11.8	18.1	17.5	15.6	18.6
$[CyOH^-]$, mol %	2.4	1.9	1.7	1.4	1.6	1.7	1.7
$[OpOH^-]/[CyOH^-]$	11.5	17.6	24.9	32.7	32.7	31.8	34.2
$[Op(OH^-)_2]_{const}$, mol %	1.4	1.4	1.8	1.9	2.8	3.6	4.2
$\Delta^*[ADP]$, mol %	3.0	2.8	2.9	1.8	2.3	2.2	2.1
$\Delta^*[AMP]$, mol %	1.4	1.8	1.9	2.6	2.7	2.6	2.5
$\Delta^*([Cy] + [CyOH^-] + Op(OH^-)_2])$, mol %	5.0	9.4	11.8	7.8	15.0	19.5	15.7
$\Delta^*([Op] + [OpOH^-])$, mol %	0.6	4.8	7.0	3.4	10.0	14.7	11.1
$(w_{in}/w_{const})_{ATP}$	2.1	2.3	2.7	2.4	3.3	3.7	3.1
$(w_{in}/w_{const})_{ADP}$	1.9	2.3	2.7	2.0	3.6	4.1	3.2
$(w_{in}/w_{const})_{AMP}$	2.5	2.1	2.6	2.8	3.3	3.5	3.1

* The symbol Δ denotes a change in the corresponding value from the moment the attainment of equilibrium in the step of $Op(OH^-)_2$ formation to the beginning of the region of constant rates. All concentrations are in mol % with respect to $[Zn \cdot ATP]_0$.

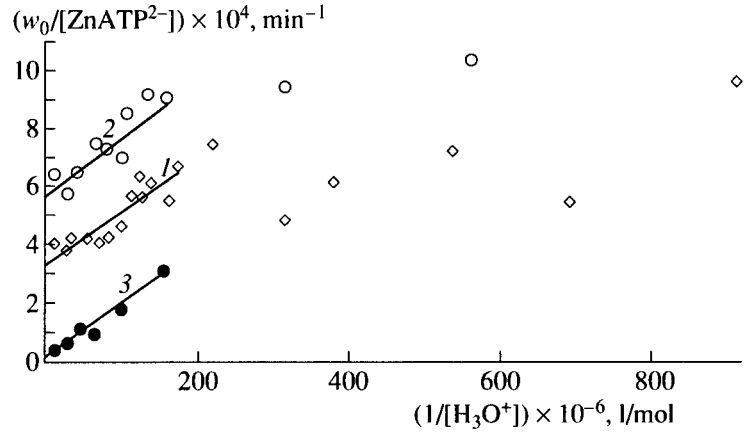

Fig. 3. The apparent rate constants of ADP formation from $ZnATP^{2-}$ $w_0/[ZnATP^{2-}]$ found from the initial rates as a function of $1/[H_3O^+]$ in three experimental series at 50°C. The experimental conditions: (*1*) $[Zn \cdot ATP]_0 = (2.74 \pm 0.04) \times 10^{-3}$ mol/l, pH 7.1–9.0; (*2*) $[Zn \cdot ATP]_0 = (4.29 \pm 0.21) \times 10^{-3}$ mol/l, pH 7.1–8.75; and (*3*) $[Zn \cdot ATP]_0 = (0.401 \pm 0.001) \times 10^{-3}$ mol/l, pH 7.1–8.2.

$[ZnATP^{2-}]_0 = [Cy]_0 + [Op]_0$. Then, the dimer concentration is

$$[D] = K_D[ZnATP^{2-}]_M^2 = K_D'[Cy]^2$$
$$\text{and } [ZnATP^{2-}]_M = [Cy](1 + b), \quad (7)$$

where the subscript M refers to the monomer.

At pH 7.1–8.2, when b is independent of pH, these linear dependences are parallel and their slope provides information on the specific rate constant k_1 of the hydrolysis of the cyclic deprotonated $CyOH^-$ species. This rate constant characterizes the pH-dependent pathway for ADP formation. The slope equals $k_1K_{a,Cy}/(1 + b)$ [43]. The dependences of $w_0/[ZnATP^{2-}]_0$ on $1/[H_3O^+]$ are linear only if we consider the initial rate of ATP consumption. The formation of intermediate AMP precursors becomes slower the equilibrium Op $\rightleftharpoons$ Cy, and the fraction of Cy among all $ZnATP^{2-}$ species decreases. The lower the $[H_3O^+]$, the earlier the stages of ADP formation at which the Op $\rightleftharpoons$ Cy equilibrium is disturbed. Figure 3 shows that, in series *1* and *2* of experiments at pH > 8.2, the ratios of the initial rates of ADP formation from $[ZnATP^{2-}]_M$ are much lower than expected, and b is higher than the value predicted by the linear dependence at an early stage of hydrolysis. Figure 3 also points to the fact that the equilibrium between Op and Cy is disturbed and that the formation of Cy from Op is slower than in a more acidic medium. On this basis, we conjecture that the transformation Op $\rightleftharpoons$ Cy is catalyzed by H_3O^+ and becomes slower in the alkali medium [44]. Our understanding of the mechanism can be summarized as follows: at an early stage of hydrolysis at pH 7.1–8.2, the slow cleavage of the P_γ–OP_β bond is a rate-determining step. At pH > 8.5, the rate of Op $\rightleftharpoons$ Cy transformation is comparable or lower than the rate of P–OP bond cleavage. At pH < 8.2, Op, Cy, $CyOH^-$, and $OpOH^-$ are in equilibrium at an early stage of hydrolysis. This equilibrium is established via steps 4 $\rightleftharpoons$ 5 $\rightleftharpoons$ 3 (see Scheme 1). Reaction 6 with OH^- disturbs the equilibrium of step 5 at an early stage of hydrolysis at pH > 8.5, and processes 10 and 11 catalyzed by the OH^- ion and reaction 7 occur in the alkali medium. The fact that the ratio $[OpOH^-]/[CyOH^-]$ = 32–34 corresponds to the segment of the kinetic curve at which the rate of ADP and AMP formation changes only slightly suggests that $CyOH^-$ transforms into $OpOH^-$ via an intermediate product. If an intermediate product were not present, the rate ADP and AMP formation would decrease in the course of the process. However, the $[OpOH^-]/[CyOH^-]$ would not be higher than 8–10. The fact that this ratio is close to 30 suggests the presence of an intermediate product $Cy'OH^-$ in a small concentration. This product slowly transforms into $OpOH^-$, and the ratio of the rate constants in the slow step becomes much higher than 8–10.

At the first step of the numerical modeling, the scheme of conformer transformations at pH > 8.5 consisted of 17 reactions and 11 species. $Op'OH^-$ was initially absent from Scheme 1 [44]. Figure 4 illustrates how the rate constants were found, which agreed with the experimental kinetic curves of ADP and AMP formation in run 3 (Table 1) at pH 8.73. The concentration of species in Fig. 4 is given in the fractions of $[NuP]_0$. In the calculations, we assumed that, at the initial moment, there is an equilibrium between Op, Cy, and D and $C_M = [Op]_0 + [Cy]_0$, $([Op]/[Cy])_0 = 2.6$. D can be neglected in the balance of $ZnATP^{2-}$ species. The initial concentration of $ZnATP^{2-}$ was calculated according to data from potentiometric titration. Using the values of $K_{a,Cy}$ and $K_{a,Op}$, we found $[CyOH^-]_0$ and $[OpOH^-]_0$. The initial concentration $[D]_0$ was determined using the value of the equilibrium constant K_D' = 179 l/mol. We used the following values of rate constants: $k_{-9} = 5$ min^{-1}

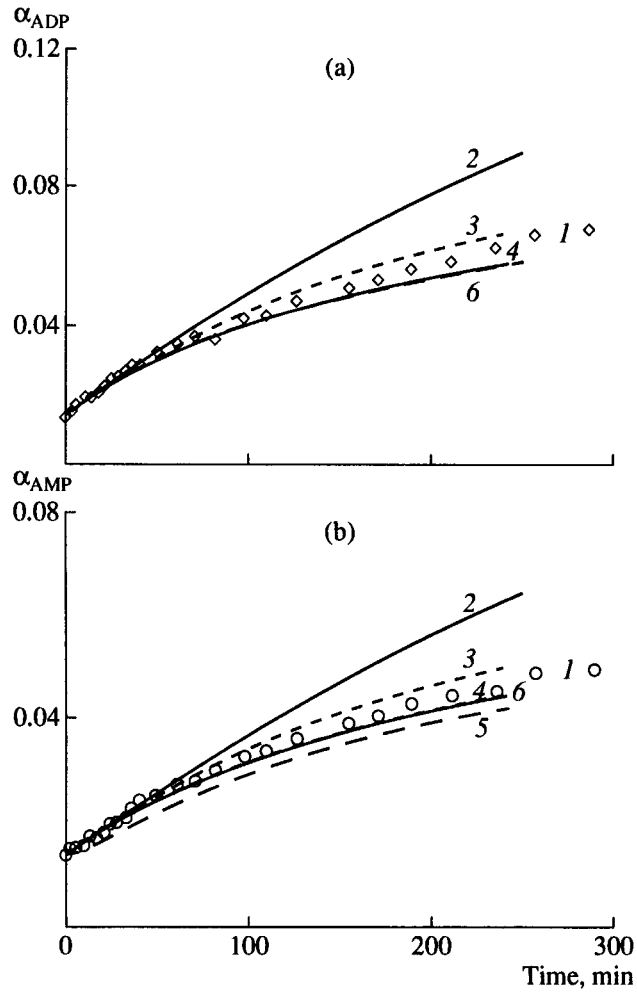

Fig. 4. Comparison of the experimental kinetic curves of (a) ADP and (b) AMP formation at pH 8.73 with the curves calculated from Scheme 1 at different values of the rate constants for steps 7 and 6. Points refer to the experimental data (variant *1*). The rate constants corresponding to variants *2–6* are given in the text.

and $k_9 = 895$ l mol^{-1} min^{-1}. Bimolecular rate constants of the ion interaction k_{-4} and k_{-3} were set equal to 6×10^{10} l mol^{-1} min^{-1} (the rate constants of diffusion-controlled processes [49]). The rate constants of the reverse reactions $k_4 = 98.4$ min^{-1} and $k_3 = 50$ min^{-1} were calculated from the equilibrium constants of ionization. In the calculations, we assumed that $k_{-10}/k_{10} = 5.7$. This rate is equal to [CyOH$^-$]/[Cy'OH$^-$], when these species are in equilibrium (the rate laws of steps 10 and –10 involve [OH$^-$]). Variant *1* in Fig. 4 represents the experimental points. Calculated variant *2* consists of 17 reactions and 11 species. In this case, $k_7 = 4 \times 10^{-2}$ min^{-1} (the rate constant of Cy'OH$^-$ transformation into OpOH$^-$); $k_{-7} = 1.3 \times 10^{-3}$ min^{-1} (this constant characterizes to the rate of OpOH$^-$ conversion); $k_6 = 2.5 \times 10^4 =$ l mol^{-1} min^{-1}; and $k_{-6} = 0.6$ min^{-1}.

In variant *3*, we also considered 17 reactions and 11 species, but the ratio $k_7/k_{-7} = 0.23$ min$^{-1}/1.3 \times 10^{-3}$ min^{-1} = 177 was much higher. In this case, the fit was much better. A further decrease in k_{-7} to 6×10^{-4} min^{-1} was unreasonable because this did not improved the fit.

In variant *4*, we considered the entire Scheme 1 in which CyOH$^-$ rapidly transforms into Cy'OH$^-$ with the participation of OH$^-$. Cy'OH$^-$ slowly transforms into Op'OH$^-$. The latter species rapidly transforms into OpOH$^-$ with the participation of OH$^-$: $k_7 = 0.23$ min^{-1}, $k_{-7} = 7.5 \times 10^{-3}$ min^{-1}, and the constants k_6 and k_{-6} are the same as in variant *2*. The values of k_7 and k_{-7}, which were used in variant *4*, were also used in all other variants.

In variants *5* and *6*, we found the values of the constants of step 6, which still better corresponded to the experimental kinetic curves: $k_6 = 2.5 \times 10^3$ l mol^{-1} min^{-1}, $k_{-6} =$ 0.06 min^{-1} for variant *5* and $k_6 = 1.25 \times 10^4$ l mol^{-1} min^{-1} and $k_{-6} = 0.3$ min^{-1} for variant *6* (the best fit). Table 3 shows the experimental and calculated values of τ_{ind} for AMP according to variants *5* and *6*. It can be seen that, given the same value of the equilibrium constant of Op(OH$^-$)$_2$ formation from CyOH$^-$ and OH$^-$ ($K'_{eq} = 4.2 \times 10^4$ l/mol), variant *5* gives the values of τ_{ind}, which are much higher than in the experiment. Variant 6 provides the best fit. The value $k_8 = 4.5 \times 10^{-3}$ min^{-1}, which adequately describes the ratio of concentrations $[ADP]_t/[AMP]_t$, was used in all further variants of calculation. In variants *4–6*, we assumed that the bimolecular rate constants of steps 10 and 11 (Scheme 1) are $k_{10} = k_{-11} = 1.4 \times 10^4$ and $k_{-10} = k_{11} = 8 \times 10^4$ l mol^{-1} min^{-1}. Assuming these values, the equilibrium in step 10 is achieved 6 times faster at pH 8.50 than the transformation of Cy'OH$^-$ into Op'OH$^-$. At the highest pH, the equilibrium is achieved 25 times faster. That is, the rate-determining step of ion isomerization is step 7. Figure 5 shows the results of analogous calculations for run 1 (Table 1, pH 8.50).

The fast formation of intermediate products (Cy'OH$^-$, Op'OH$^-$, and Op(OH$^-$)$_2$) at an early stage of hydrolysis and a rather high value of the rate constant of the transformation of Cy'OH$^-$ into Op'OH$^-$ (0.23 min^{-1}) lead to a drastic decrease in the concentration of the cyclic species at high pH from the reaction start. This explains the fact that inactive OpOH$^-$ species dominate among the ZnATP^{2-}OH$^-$ species, as is evident from the ^{1}H$^-$ NMR spectra of Zn^{2+} and Cd^{2+} complexes with ATP^{4-} at high pH [29, 30].

Scheme 1a shows the assumed mechanism of the isomeric transformation of ions CyOH$^-$ $\rightleftharpoons$ OpOH$^-$. Step 10 (Scheme 1) is the addition of the OH$^-$ ion of the medium to the γ-phosphate group of the monomeric CyOH$^-$ species. As this takes place, the OH$^-$ group bound to Zn^{2+} in the reaction center is displaced and escapes to the medium. A pentacovalent intermediate is formed (at the γ-P atom). During the formation of

Cy'OH$^-$, the protonation state of groups bound to γ-P probably changes, and H$^+$ is at the O$^-$ atom belonging to the terminal phosphate, whereas the OH group is at the equatorial position with respect to γ-P. The consideration of the spatial model shows that both OH$^-$ ions (at γ-P and Zn^{2+}) cannot be located in the same reaction center. Then, pseudotransformation follows (the bridging P_γ–OP_β bond is a pivot for pseudotransformation), which is a rate-determining step in the sequence of steps of ion isomerizations 10 ⇌ 7 ⇌ 11. The rate constants k_7 and k_{-7} are independent of pH within the pH range studied. The OH$^-$ group appears in the apical position relatively to the γ-P. Then, the OH$^-$ ion attacks Zn^{2+} of the pentacovalent intermediate of the open species in step 11, and the OH$^-$ group of the γ-phosphate escapes to the medium. The rate constant of the pseudotransformation of the strained Cy'OH$^-$ molecule to species Op'OH$^-$ (0.23 min^{-1}) is 30 times higher than the rate constant of the reverse reaction. The concept of pseudotransformation is widely used to explain the formation of products of the acid-catalyzed hydrolysis of oxygen-containing cyclic ethers of phosphorous [50]. The role of pseudotransformation in cyclization/clearage reactions (the cleavage of dinucleotide uridyl(3',5')uridine ((3',5")UpU) catalyzed by an imidazole buffer has also been established. The cleavage of the 3'–5"-phosphodiether bond to form uridine 2',3'-cyclophosphate and 5"-nucleoside (uridine) occurs via a sequential bifunctional mechanism, according to which one of the components of the buffer catalyzes the formation of a phosphorane intermediate and the other component catalyzes its decomposition into the products. In the formation of the pentacovalent intermediate (cyclization), the 2'-hydroxyl group of ribose attacks the 3',5"-phosphodiether group. During further cleavage of the 3'–5"-ether bond, uridine 2',3'-cyclophosphate is formed. Along with cleavage, the isomerization of (3',5")UpU into (2',5")UpU occurs, which involves the pseudotransformation of the pentacovalent intermediate. During this process, the ether group 2'–O–P changes from apical position relatively to P to the equatorial position and a change for the 3'–O–P group has a backward direction. Further protonation of the 3'-O position in the phosphorane catalyzed by the imidazolium ion results in the formation of the (2',5")UpU isomer [51, 52]. The 2',3'-cyclophosphate intermediate is formed in the catalysis by ribonuclease as well.

Inclusion of the pH-Independent Pathway of Hydrolysis within the Framework of the Dimeric Model

A more complicated kinetic scheme (Scheme 2) accounts for the pH-independent hydrolysis pathway. This scheme consists of 43 constants and 27 species and considers only dimeric ZnATP^{2-} associates. Figure 6 shows how the concentrations of intermediate products change during hydrolysis at high pH as calculated according to Scheme 2.

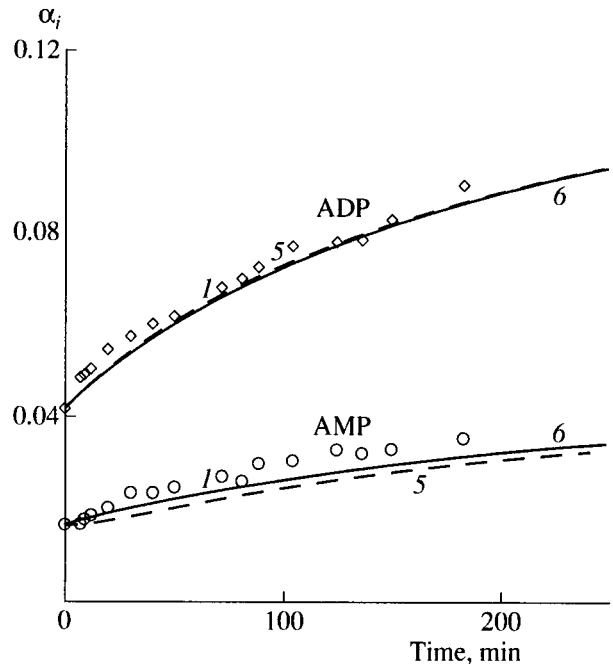

Fig. 5. Comparison of the experimental kinetic curves of ADP and AMP formation at pH 8.50 with the curves calculated by Scheme 1 at different values of the rate constants for step 6. Points refer to the experimental data (variant *1*). Curves *5* and *6* were calculated by the corresponding variants.

Figures 6 and 7 compare the experimental kinetic curves of ADP and AMP formation to the curves simulated with Scheme 2. For pH 7.1, analysis of the concentration dependences for the pH-independent hydrolysis pathway of the dimeric $(ZnATP^{2-})_2H^+OH^-$ complex consisting of two monomeric cyclic molecules (see Fig. 1c) was performed within the framework of Scheme 2, assuming that the hydrogen bond N1···H$^+$···O$^-$–P_γ is formed and that equilibrium is attained between the open forms of ZnATP^{2-}, Cy(ZnATP^{2-}), and the dimer at an early stage of hydrolysis. The detailed description of this analysis will be reported elsewhere. According to the above assumptions for the calculations according to Scheme 2, we used the rate constants k_9 = 1300 l mol^{-1} min^{-1} (proton transfer with the formation of a hydrogen bond) and k_{-9} = 5 min^{-1} (for the reverse reaction). These constants were estimated for the range of Zn · ATP concentrations between 2.7×10^{-3} and 0.27 mol/l at pH 7.1. The equilibrium constant K'_D = 260 corresponds to the value $K_D \approx 20$ if it formally refers to the unit monomer concentration. This analysis was performed assuming that the slow step of dimer hydrolysis with ADP formation is the transfer of H$^+$ that participates in the formation of the hydrogen bond N1···H$^+$···O$^-$–P_γ to the hydrogen bond N1···H$^+$···O$^-$–P_β of the ZnADP$^-$ formed (step 2, $k_2 = 1.2 \times 10^{-2}$ min^{-1}). This value of the rate constant was

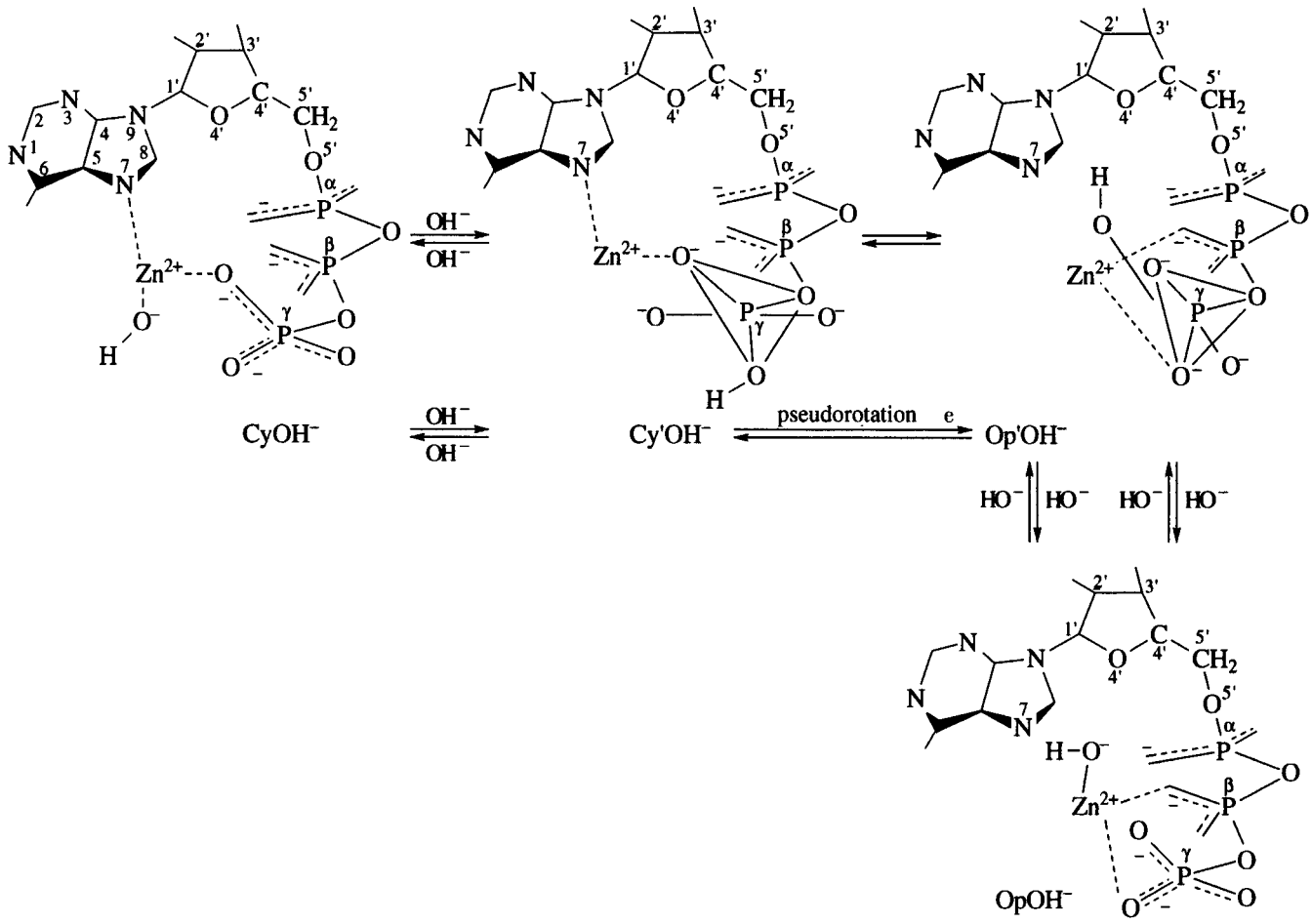

Scheme 1a

used in all calculations according to Scheme 2 as the best found value for the description of the concentration dependence for the pH-independent pathway of dimer hydrolysis at pH 7.1 and for the description of the pH dependence of ADP formation kinetics on pH at pH 7.1–8.2 and $[Zn \cdot ATP]_0 = (2.74 \pm 0.04) \times 10^{-3}$ (series *I*) and $(4.29 \pm 0.21) \times 10^{-3}$ (series *II*). In the intermediate complex D'{Cy(ZnADP$^-$) · Cy(ZnATP^{2-})H$^+$(HPO_4^{2-})}, the bridging bond between P_γ and OP_β is cleaved. Then, the fast reversible substitution of the ligand at Zn^{2+} occurs: HPO_4^{2-} abstracts H^+ from the hydrogen bond and cleaves it; then the $H_2PO_4^-$ ligand at Zn^{2+} is substituted for H_2O (step 16). As a result of these processes, the K(ADP) complex is formed in which Cy(ZnADP$^-$) and the catalyst Cy(ZnATP^{2-}) are only bound by stacking interaction, the phosphate chain ZnADP$^-$ is hydrated, and $H_2PO_4^-$ escapes to the aqueous medium. The K(ADP) complex is in equilibrium with Cy(ZnADP$^-$) and Cy(ZnATP). Their interaction with the formation of K(ADP) (step 17) is controlled by diffusion. In general, hydrolysis with the formation of ADP and P_i, in which the N1 atom of the second molecule plays the role of a general base catalyst, is considered as a reversible process as every H^+ transfer with the participation of a hydrogen bond. Under our experimental conditions (the conversion of ATP is 10–20%, the initial concentration of P_i is low and an aqueous medium), the slight reversibility was taken into account at pH 7.1 only at very high concentrations of Zn · ATP. It is clear from Scheme 2 that the following factors are favorable for the reverse reaction: a high concentration of P_i, a weakly acidic medium (P_i is in the form $H_2PO_4^-$, whereas the fraction of $H_2PO_4^-$ in the balance of P_i species is ≤ 0.05 at pH $\leq$ 8.5), and a low thermodynamic activity of water (the rate law of step –16 involves $[H_2O]$). The transformation of $H_2PO_4^-$ into HPO_4^{2-}, the ionization of Cy and Op forms of ZnADP$^-$, and a decrease in the concentration of Zn · ATP make the formation of ADP completely irreversible. Thus, at pH $\leq$ 8.5 (see Table 1), the formation of ADP is completely irreversible.

Scheme 2 takes into account the fact that dimer hydrolysis via the pH-independent pathway produces

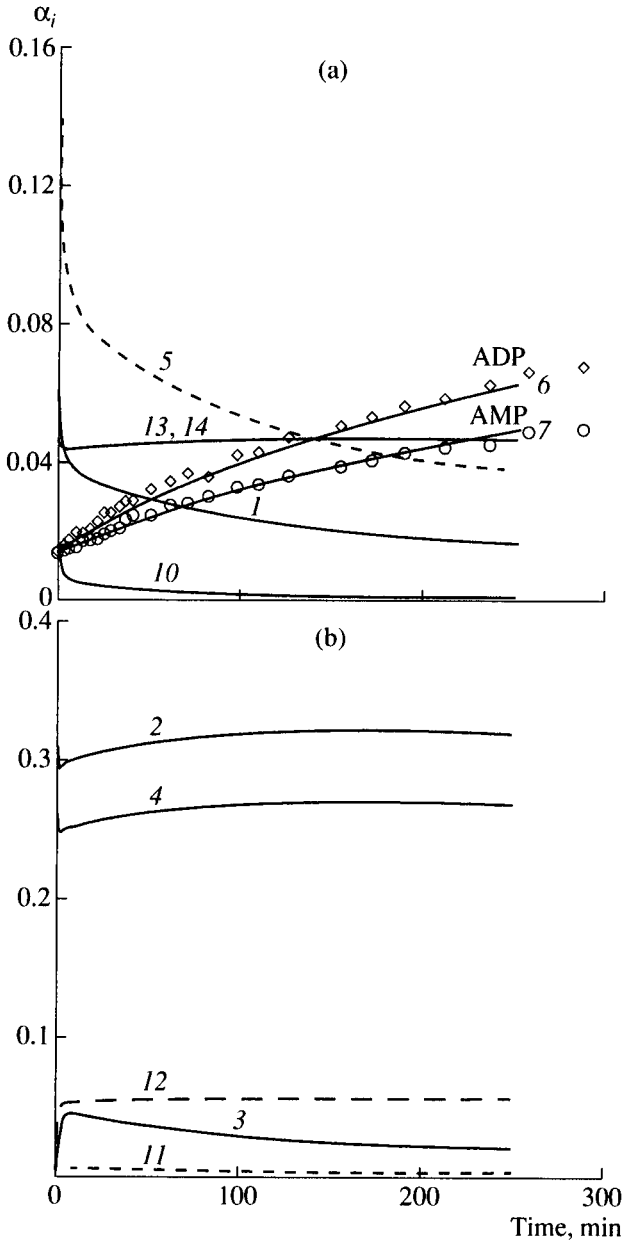

Fig. 6. Variation in the relative concentrations of intermediate products during hydrolysis at pH 8.73 and 50°C (run 3, Table 1): (*1*) $CyOH^-$, (*2*) $OpOH^-$, (*3*) $Op(OH^-)_2$, (*4*) Op, (*5*) Cy, (*6*) ADP, (*7*) AMP, (*10*) D, (*11*) $Cy'OH^-$, (*12*) $Op'OH^-$, (*13*) Op', and (*14*) Op". The concentrations α_i are expressed in molar fractions of $[NuP]_0$. Points refer to the experimental concentrations of ADP and AMP. The calculations were performed according to Scheme 2 using the dimeric model. The rate constants of separate steps are given in the text.

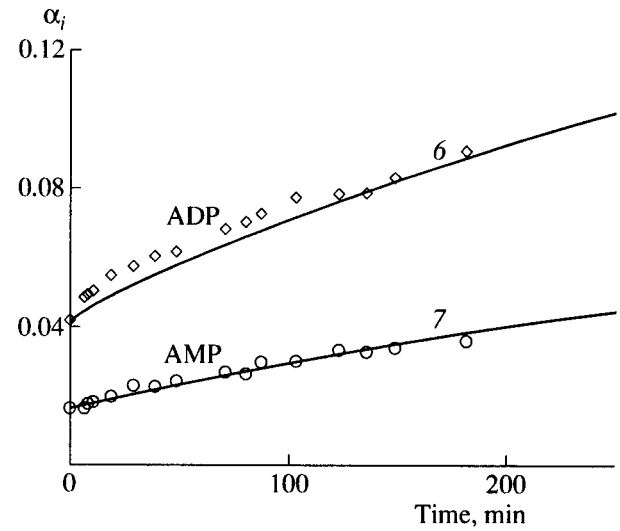

Fig. 7. Experimental kinetic curves of ADP and AMP formation (points) at pH 8.50 and 50°C (run 1, Table 1) and the corresponding curves calculated according to the dimeric model within the framework of Scheme 2 (lines).

AMP in parallel with ADP. Analysis of hydrolysis kinetics at pH 7.1 allowed us to suggest that AMP is formed from the intermediate $(DOH^-)H^+$ product formed from the dimer D by the substitution of the OH^- ion bound to Zn^{2+} in the opposite position to the γ-phosphate group (Fig. 1c) by another OH^- ion, which is bound to Zn^{2+} in the opposite position to the β-phosphate group (step 14). The intermediate product $(DOH^-)H^+$ then slowly decomposes via step 15 into AMP and pyrophosphate PP_i. As this takes place, the $Cy(ZnATP^{2-})$ molecule is liberated, which acts as a general base catalyst for dimer hydrolysis. By contrast to Scheme 1, Scheme 2 contains the steps of $Cy(ZnATP^{2-})$ formation from $Op(ZnATP^{2-})$. We assume that the formation of Cy from Op occurs via three steps (Scheme 2a). In the first step, which is very fast, H_3O^+ participates in the cleavage of the hydrogen bond between the hydrated water molecule and terminal phosphate to form a pentacovalent intermediate with the γ-P atom (Op'). This intermediate contains two OH groups. The OH^- ion added from the medium is in the apical position relatively to γ-P. Then, fast pseudotransformation occurs, and the Op" is formed in which OH^- from the medium appears in the equatorial position relatively to γ-P, and the OH group of the phosphate holds the apical position. Then, in the slow step with the participation of the H_3O^+ ion, the OH group leaves the apical position and forms the coordinated water molecule, and the terminal phosphate is hydrated to form $Cy(ZnATP^{2-})$. This scheme explains a decrease in the rate of the Op $\rightleftharpoons$ Cy isomerization observed at pH > 8.5. In the calculation according to Scheme 2, we assumed that the Op species dominates in the sum of the concentrations of the open species (ΣOp = [Op] + [Op'] + [Op"]), and the $OpOH^-$ ions are formed from Op. The concentrations of Op', Op", and Cy are commensurate (the ratio of forms under equilibrium conditions at zero time is proposed to be [Op] : [Op'] : [Op"] : [Cy] = 5.7 : 1 : 1 : 2.9, $(\Sigma[Op]/[Cy])_0 = 2.66$, and $[OpOH^-][H_3O^+]/\Sigma[Op] = 1.64 \times 10^{-9}$ mol/l). Because the fraction of the Op species, which is ionized to form $OpOH^-$, is $0.74\Sigma[Op]$, the equilibrium constant of Op

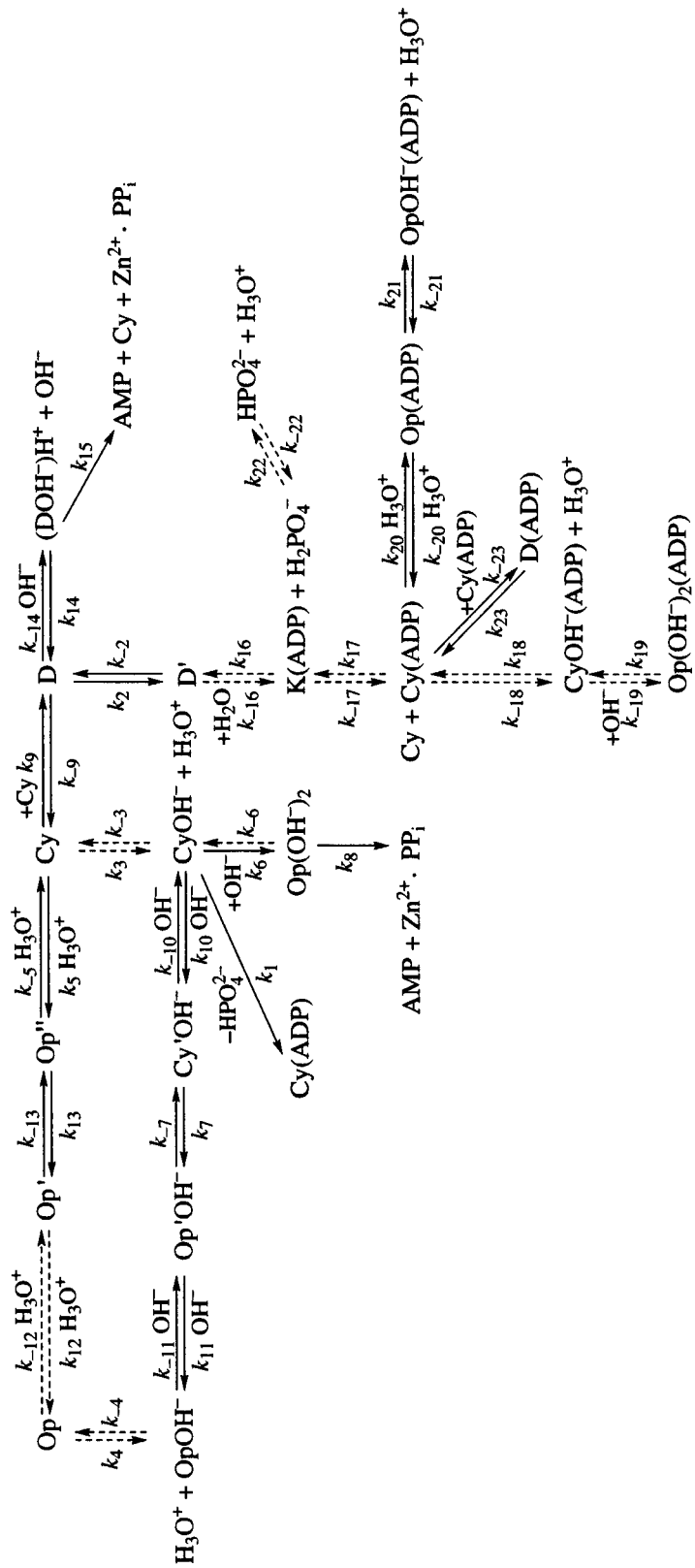

Scheme 2

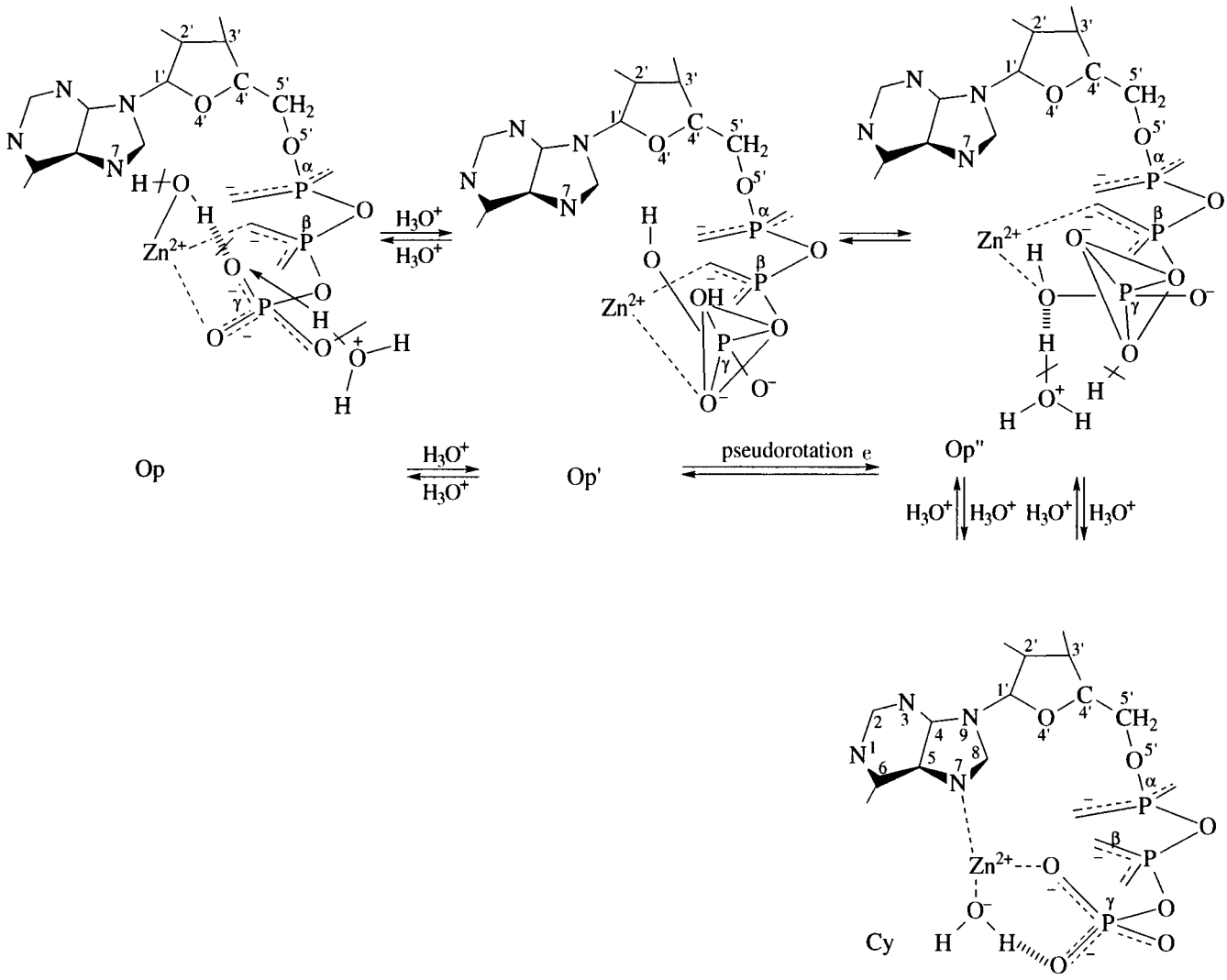

Scheme 2a

ionization used in the calculations changes to $K_{a,Op} = 2.21 \times 10^{-9}$ mol/l and, correspondingly, $k_4 = 133$ min^{-1}. The balance equation at the initial moment, when Op, Op', Op", Cy, and D are in equilibrium, takes the following form in the calculations within the framework of Scheme 2: $[ZnATP^{2-}]_0 = (\Sigma[Op])_0 + [Cy]_0 + 2K'_D[Cy]_0^2$. In this equation, the sum of the first two terms is equal to the monomer concentrations, and the third term accounts for the dimer. Taking into account the above expressions and the value $K'_D = 260$, we have

$$[ZnATP^{2-}]_0 = 3.66[Cy]_0 + 2 \times 260[Cy]_0^2. \quad (8)$$

The concentration of $ZnATP^{2-}$ is in mol/l. Expression (8) was input into the program and the initial concentrations $[Cy]_0$, $[Op]_0$, $[Op']_0$, $[Op"]_0$, $[OpOH^-]_0$, $[CyOH^-]_0$, and $[D]_0$ were found taking into account formula (8) (see Appendix). The changes in the concentrations of all intermediate products were calculated using the rate constants assigned to each step. The numerical values of the main rate constants, which provide the best fit of the kinetics of ADP and AMP formation at pH 7.1 and pH-dependence at pH 7.1–8.2 within the framework of the dimeric model, are as follows: $k_2 = 1.2 \times 10^{-2}$ min^{-1}, $k_{-5} = 5.8 \times 10^6$ l mol^{-1} min^{-1}, $k_5 = 2 \times 10^6$ l mol^{-1} min^{-1}, $k_{-12} = 1.4 \times 10^8$ l mol^{-1} min^{-1}, $k_{12} = 8 \times 10^8$ l mol^{-1} min^{-1}, $k_{-16}[H_2O] = 5$ min^{-1}, $k_{16} = 10^4$ l mol^{-1} min^{-1}, $k_{-13} = k_{13} = 0.25$ l mol^{-1} min^{-1}, $k_{-14} = 1.2 \times 10^4$ l mol^{-1} min^{-1}, $k_{14} = 4 \times 10^3$ l mol^{-1} min^{-1}, $k_{15} = 2 \times 10^3$ min^{-1}, $k_{-22} = 6 \times 10^{10}$ l mol^{-1} min^{-1}, $k_{22} = 3.79 \times 10^3$ min^{-1}, $k_{17} = 6 \times 10^{10}$ l mol^{-1} min^{-1}, and $k_{-17} = 1.2 \times 10^{10}$ min^{-1}. The rate constants of steps 3 and 4 (except for k_4), 10, 11, 7, 1, 6, and 8 were taken from Scheme 1.

Figure 8 illustrates fitting the constants k_5 and k_{-5} to the kinetic curves of ADP and AMP formation in the alkali medium. The pH 8.7–9.0 range is the most sensitive to the values of these constants, because the equi-

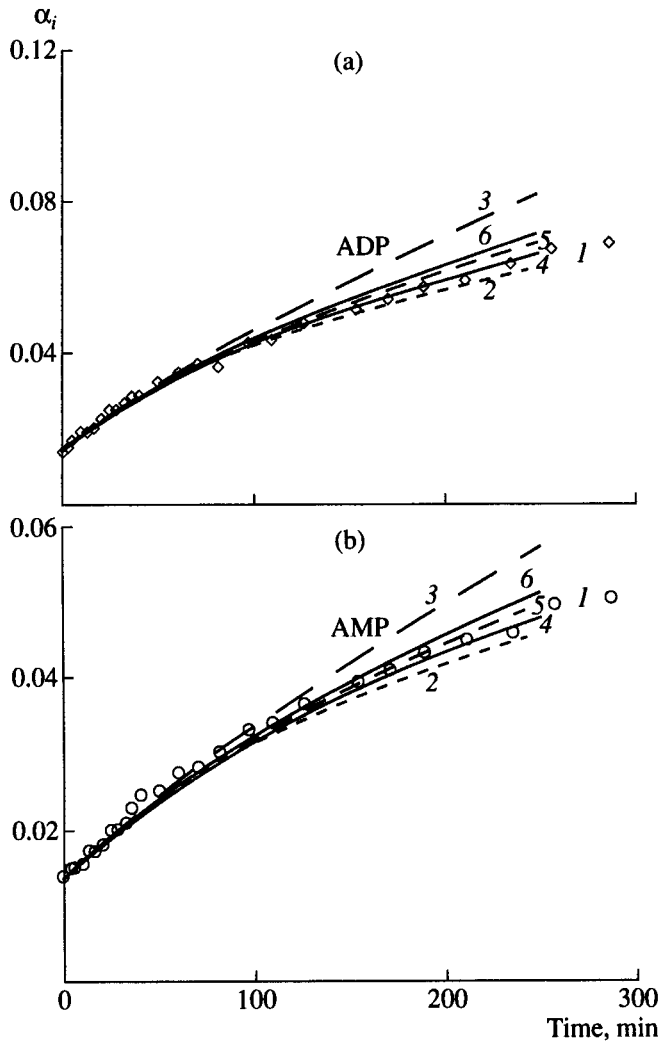

Fig. 8. Comparison of the experimental kinetic data of (a) ADP and (b) AMP formation at pH 8.73 with the curves calculated according to Scheme 2: (*1*) experiment; (*2*) $k_{-5} = 2.9 \times 10^6$ min^{-1}, $k_5 = 1 \times 10^6$ min^{-1}; (*3*) $k_{-5} = 2.9 \times 10^7$, $k_5 = 1 \times 10^7$; (*4*) $k_{-5} = 5.8 \times 10^6$, $k_5 = 2 \times 10^6$, (*5*) $k_{-5} = 8.7 \times 10^6$, $k_5 = 3 \times 10^6$; (*6*) $k_{-5} = 1.16 \times 10^7$, $k_5 = 4 \times 10^6$ (all constants are in l mol^{-1} min^{-1}).

librium of step 5 is disturbed due to a low concentration of H_3O^+ (the rate laws of reactions 5 and –5 include $[H_3O^+]$). All other constants were kept invariable when fitting k_5 and k_{-5}. The curves of ADP and AMP formation calculated according to variant *2* are lower, and those calculated according to variant *3* are noticeably higher than the experimental curves. The best fit is achieved in variant *4* ($k_{-5} = 5.8 \times 10^6$ l mol^{-1} min^{-1} and $k_5 = 2 \times 10^6$ l mol^{-1} min^{-1}). The range of admissible values is $(8.7–2.9) \times 10^6$ l mol^{-1} min^{-1} for k_{-5} and $(3–1) \times 10^6$ l mol^{-1} min^{-1} for k_5. Analogous calculations for runs 5 (pH 8.96) and 6 (pH 9.02) (Table 1) led to the same conclusion, and we used the values corresponding to variant *4* in all further calculations.

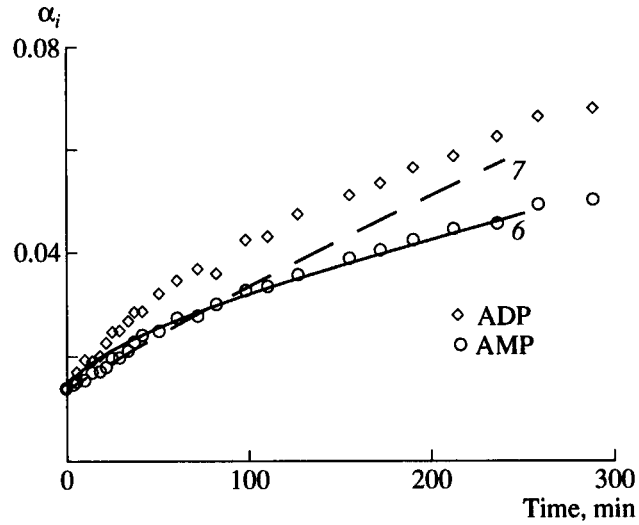

Fig. 9. Anomalous kinetic curves of (*6*) ADP and (*7*) AMP formation calculated assuming the addition of an extra OH^- ion rather than a change in the OH^- position in the reaction center takes place in the formation of the intermediate from the dimer in step 14. Points refer to the experimental data.

Figure 9 shows the calculations for run 3 assuming that step 14 is $D + OH^- \rightleftharpoons DOH^-$. We used the same rate constants as in Figs. 6 and 7 ($k_{-14} = 1.2 \times 10^4$ l mol^{-1} min^{-1}). However, we assumed that, for the reverse reaction, the rate constant of the pseudo-first order is the same as at pH 7.1 ($k_{14}[OH^-] = 0.003$ min^{-1}). That is, the rate law of step 14 in the reverse direction does not contain $[OH^-]$. This assumption had to be checked because the monomeric species $Op(OH^-)_2$ was formed by the addition of the second OH^- ion to $CyOH^-$, and this second ion substitutes N7 in the coordination sphere of Zn^{2+} [43, 44]. Figure 9 shows anomalous curves of ADP (curve *6*) and AMP (curve *7*) formation, which contradict the experimentally determined parallel formation of ADP and AMP during the process. Analysis of the three last rows in Table 5 shows that the rate law of ATP consumption and ADP and AMP formation during the process is the same at constant pH. Similar calculations enabled us to exclude the formation of AMP in the associate via an intermediate product formed by the addition of the second OH^- ion. Scheme 2, which assumes the direct substitution of OH^- opposite to γ-P by OH^- opposite to β-P in the reaction center of the dimer, was used in all subsequent calculations.

The values of rate constants of separate steps found within the framework of the dimeric model allow the quantitative estimation of the reasons for a decrease in the reaction rate in the course of the process at pH > 8.5 (Table 5). Table 6 shows the calculated concentration profiles for some intermediate products (in molar fractions of $[NuP]_0$) and the formation rates for the species that are active in hydrolysis compared to the rates of hydrolysis product formation (ADP and AMP) in runs

Table 6. The rates of formation of species that are active in hydrolysis (Cy, $CyOH^-$, $D(Cy_2)$, and $Op(OH^-)_2$) calculated according to the dimeric model (Scheme 2), the rates of ADP and AMP formation, and the rate of the isomerization $Cy'OH^- \rightleftharpoons Op'OH^-$

pH	8.73			8.96			9.02		
Time, min	6 (τ_{ind})	100	200	4 (τ_{ind})	100	200	4 (τ_{ind})	100	200
α_{Cy}	0.089	0.0535	0.0409	0.0572	0.0291	0.0209	0.0471	0.0239	0.0172
$\alpha_{Op''}$	0.044	0.0467	0.0470	0.0358	0.0356	0.0356	0.0326	0.0321	0.0320
α_{Op}	0.251	0.268	0.270	0.195	0.208	0.208	0.177	0.188	0.187
$(w_{Op'' \rightarrow Cy} - w_{Cy \rightarrow Op''}) \times 10^7$, mol l^{-1} min^{-1}	4.07	8.63	10.18	2.92	4.60	5.11	2.58	3.75	4.09
α_{CyOH^-}	0.040	0.0239	0.0183	0.0435	0.0221	0.0159	0.0411	0.0209	0.0150
α_D	0.0057	0.0021	0.0012	0.0024	0.0006	0.0003	0.0017	0.0004	0.0002
$\alpha_{Op(OH^-)_2}$	0.0445	0.0293	0.0222	0.0751	0.0460	0.0328	0.0834	0.0499	0.0356
α_{OpOH^-}	0.298	0.319	0.321	0.395	0.421	0.421	0.410	0.435	0.434
$(w_{CyOH^- \rightarrow ADP} + w_{D \rightarrow ADP} + w_{Op(OH^-)_2 \rightarrow AMP}) \times 10^7$, mol l^{-1} min^{-1}	15.51	9.17	6.87	19.08	10.50	7.46	19.4	10.68	7.61
$\alpha_{Cy'OH^-}$	0.0066	0.0040	0.0031	0.0074	0.0038	0.0028	0.0070	0.0036	0.0026
$\alpha_{Op'OH^-}$	0.0526	0.0560	0.0564	0.0693	0.0738	0.0738	0.0720	0.0762	0.0760
$(w_{Op'OH^- \rightarrow Cy'OH^-} - w_{Cy'OH^- \rightarrow Op'OH^-}) \times 10^7$, mol l^{-1} min^{-1}	−31.78	−14.1	−8.07	−33.8	−8.98	−2.26	−30.7	−7.30	−0.93

3, 5, and 6 (Table 1). The rate of the isomerization $Cy'OH^- \rightleftharpoons Op'OH^-$ is also included in Table 6. These data refer to three moments of time: the end of the induction period, 100 min, and 200 min. The value $w_{Op'' \rightarrow Cy} - w_{Cy \rightarrow Op''}$ corresponds to the rate of $Cy(ZnATP^{2-})$ formation in step 5, which is a precursor of the dimer and $CyOH^-$ formed in a fast ionization step; $w_{CyOH^- \rightarrow ADP} + w_{D \rightarrow ADP} + w_{Op(OH^-)_2 \rightarrow AMP}$ is the sum of the rates of ADP and AMP formation; and $w_{Op'OH^- \rightarrow Cy'OH^-} - w_{Cy'OH^- \rightarrow Op'OH^-}$ is the difference between the rates of pentacovalent intermediate isomerization in the forward and reverse directions ($Op'OH^- \rightleftharpoons Cy'OH^-$). These intermediates are in fast equilibrium with $OpOH^-$ and $CyOH^-$. At an early stage of hydrolysis, when the rate of ADP formation decreases, the sum of the rates of ADP and AMP formation is much higher than the rate of Cy formation in step 5. During the process, this difference becomes less pronounced. The difference between the rates of the forward and reverse reactions $Op'OH^- \rightleftharpoons Cy'OH$ is always negative. That is, the concentration of $Cy'OH^-$ formed in step 7 (and hence the concentration of $CyOH^-$) always decreases. Therefore, $CyOH^-$ is consumed rather than formed in this step. This is one of the main reasons for a decrease in the rates of ADP and AMP formation during the process. The absolute value of the difference between the rates of forward and reverse in step 7 also decreases during the process. The slow formation of $Cy(ZnATP^{2-})$ in step 5 with the rate law containing $[H_3O^+]$ in the forward and reverse directions limits the formation of ADP and AMP. The contribution of the pH-independent pathway of dimer hydrolysis $w_{D \rightarrow ADP}$ at pH 8.73 is ~20% at the early stages and at least 10% at the final stages. At higher pH, the contribution of the dimer to ADP formation is at least 5% at the initial stage. The kinetics of ADP and AMP formation at pH > 8.8 is determined by the monomeric species transformation.

Calculations Taking into Account the Role of Trimeric $ZnATP^{2-}$ Associates

The kinetic scheme was further made more complex after analysis of the dependence of the hydrolysis rate via the pH-independent hydrolysis pathway at pH 7.1

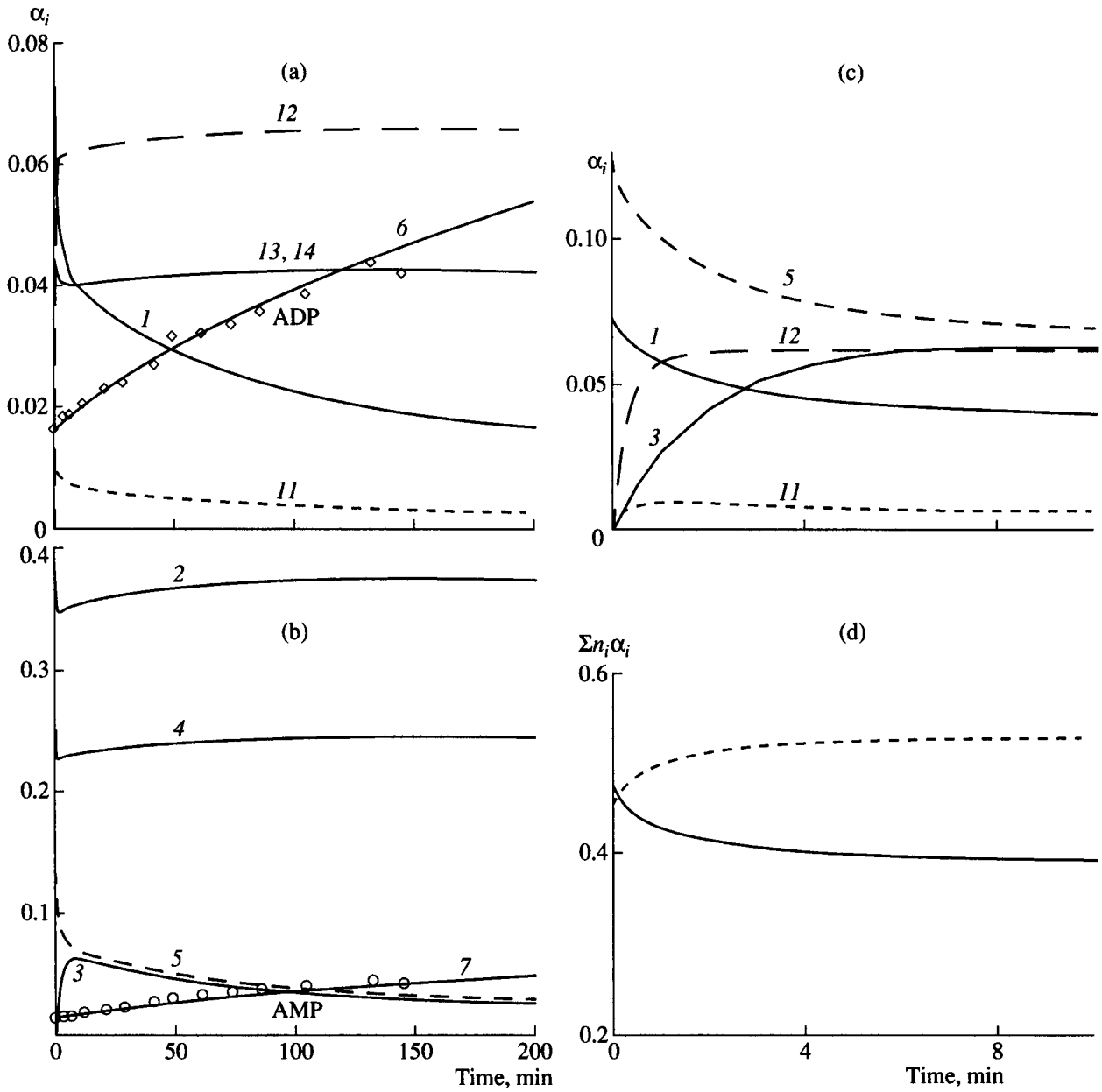

Fig. 10. Variation in (a–c) the concentration of intermediate products and (d) the overall concentration of ions and $ZnATP^{2-}$ molecules during hydrolysis at pH 8.84 and 50°C (run 4, Table 1): (*1*) $CyOH^-$, (*2*) $OpOH^-$, (*3*) $Op(OH^-)_2$, (*4*) Op, (*5*) Cy, (*6*) ADP, (*7*) AMP, (*11*) $Cy'OH^-$, (*12*) $Op'OH^-$, (*13*) Op', and (*14*) Op". The concentrations are given in molar fractions of [NuP]. Points refer to the experimental concentrations of ADP and AMP. The calculation was performed within the framework of Scheme 3 based on the trimeric model. Figures (c) and (d) refer to the first 10 min after the reaction start. The solid line in figure (d) is the overall concentration of $ZnATP^{2-}$. The dashed line is the overall concentration of ions.

on the concentration and its dependence on pH at pH 7.1–8.2. The dimeric model fails to account for the experimental series at pH 7.1–8.0 and $[Zn \cdot ATP]_0 = 4 \times 10^{-4}$ mol/l. The experimental rates of ADP formation were noticeably lower than the calculated rates. For the quantitative estimates of this effect, we considered a model in which reaction 9 in Scheme 2 was separated into two steps: two molecules of the monomeric cycle $Cy(ZnATP^{2-})$ species, the K(ATP) complex by stacking interaction in the first step and H^+ transfers with the participation of N1 in the second step. To describe the reaction kinetics at low Zn · ATP concentrations (4×10^{-4} mol/l), the formal equilibrium constants of dimer formation from two Cy molecules should be an order of magnitude lower than the corresponding constants at high $[Zn \cdot ATP]_0$ (0.14 mol/l). The rate constants of proton transfer (k_9) at low concentrations should be more than two orders of magnitude lower than at high concentrations. The calculations showed that the active dimer is formed rather slowly, and the assumption of its

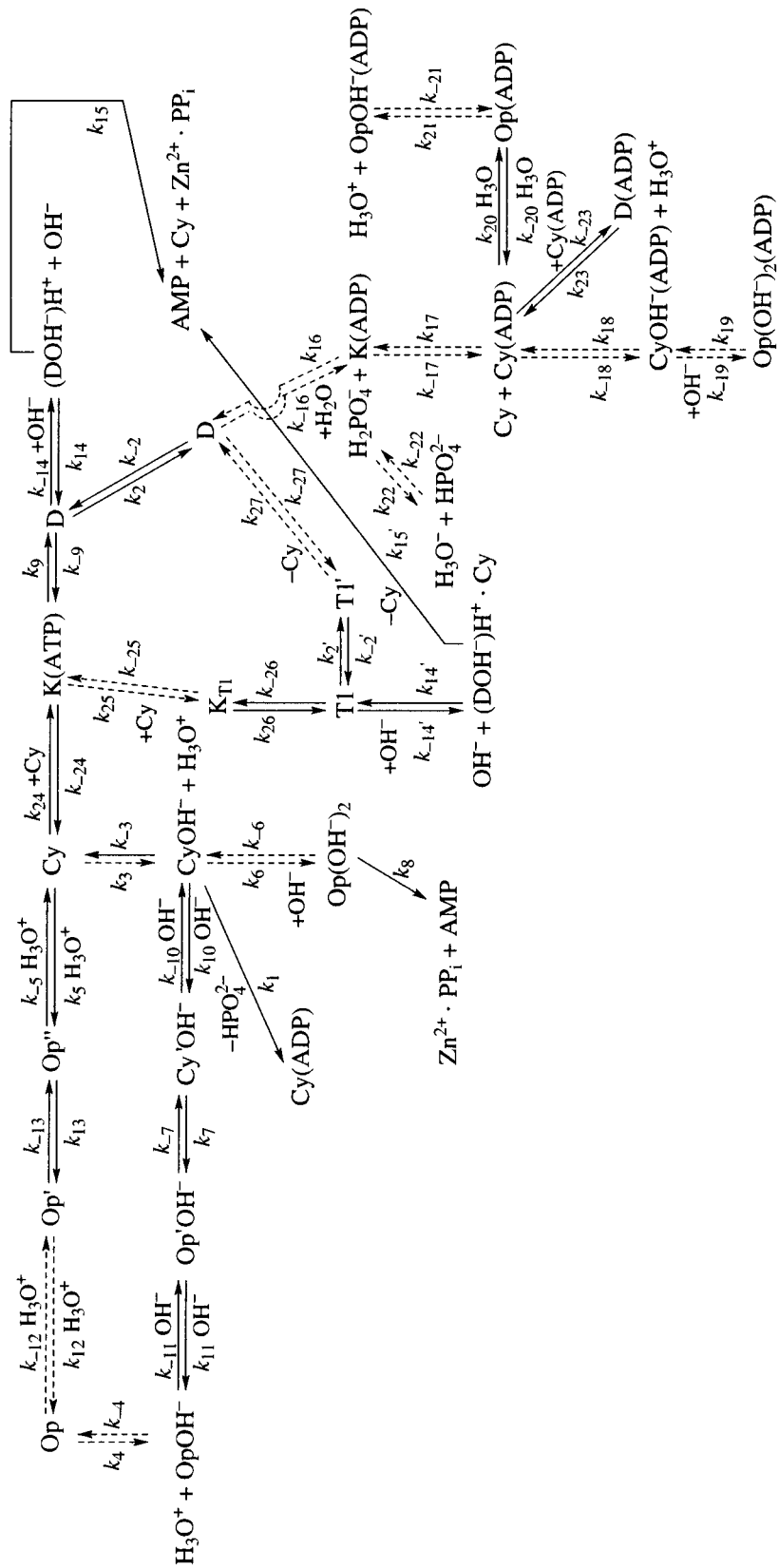
Op
Op'
Op''
Op'OH⁻
H₃O⁺ + OpOH⁻
Cy
CyOH⁻ + H₃O⁺
Cy'OH⁻
Op(OH⁻)₂
Zn²⁺ · PPᵢ + AMP
Cy(ADP)
–HPO₄²⁻
K(ATP)
AMP + Cy + Zn²⁺ · PPᵢ
D
(DOH⁻)H⁺ + OH⁻
K_T1
T1
T1'
OH⁻ + (DOH⁻)H⁺ · Cy
H₃O⁻ + HPO₄²⁻
–Cy
H₂PO₄⁻ + K(ADP)
+H₂O
H₃O⁺ + OpOH⁻(ADP)
Op(ADP)
Cy + Cy(ADP)
+Cy(ADP)
D(ADP)
CyOH⁻(ADP) + H₃O⁺
+OH⁻
Op(OH⁻)₂(ADP)

Scheme 3

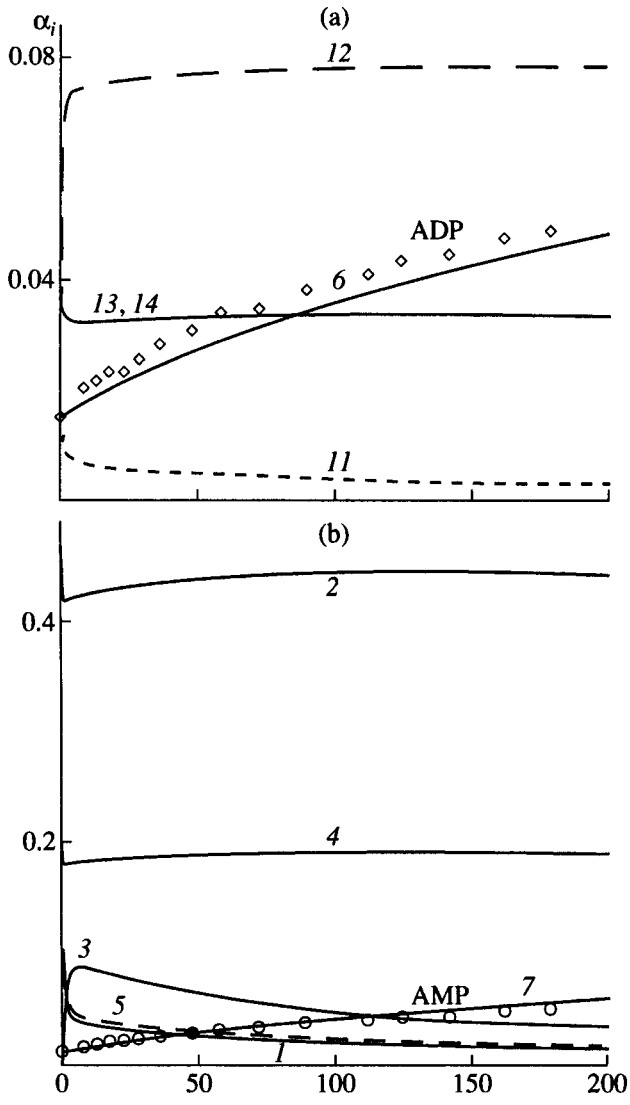

Fig. 11. Variation in the concentrations of intermediates during hydrolysis at 9.02 and 50°C (run 6, Table 1). The calculation was performed according to Scheme 3. The notation is the same as for Fig. 10.

fast formation, which was made for Scheme 2, is incorrect. To avoid this contradiction, we developed a model that takes into account the role of trimeric associates of $ZnATP^{2-}$ in the formation of species that are active in hydrolysis. Scheme 3 assumes that the dimeric complexes of two molecules Cy–K(ATP) and trimeric associates $K_{(T1)}$ and $K_{(T2)}$ are formed at an early step of hydrolysis at high rates controlled by diffusion [49]. In trimeric associates, the third molecule (Cy in $K_{(T1)}$ and Op in $K_{(T2)}$) is added via stacking interaction. The rate constant k_{26} of proton transfer in trimers with the formation of a hydrogen bond is three orders of magnitude higher than in dimers. The equilibrium constant of proton transfer in step 26 is more than 30 times higher than in the case of the dimer (step 9). The reason for an increase in the amount of active centers for hydrolysis in T1 and T2 trimers is the spatial arrangement of the third $ZnATP^{2-}$ molecule: the coordinated water from the third $ZnATP^{2-}$ stabilizes the coordinated OH^- ion of the first $ZnATP^{2-}$ molecule by forming a hydrogen bond with this OH^-. Trimers are responsible for the same processes as dimers: they form the T' complexes in a slow step 2' by H^+ transfer to β-phosphate and lose the third $ZnATP^{2-}$ molecule (Op or Cy) in a subsequent fast step. As result, D' is formed. Also, like dimers, trimers substitute the OH^- ion at Zn^{2+} to form $(DOH^-)H^+ \cdot$ Cy (or Op) complexes. Then, these complexes lose Cy (or Op) to form AMP + Cy + $Zn^{2+} \cdot PP_i$ in a slow step. The rate constants in the case of trimers are higher than in the case of dimers. For simplicity, Scheme 3 shows these processes only for T1. At moderate $[Zn \cdot ATP]_0$ concentrations (see Table 1), the role of trimers is comparable with the role of dimers in the creation of active centers for ADP and AMP formation. The calculations by schemes 2 and 3 lead to similar results at pH > 8.8 because kinetics is mainly determined by monomeric forms. The procedure of rate constant estimation in the model that accounts for trimers at pH 7.1–8.2 will be described in detail elsewhere. Figure 10 (a and b) shows how the concentrations of the main intermediate products change during hydrolysis at pH 8.84. The calculation was performed according to Scheme 3 that consists of 67 rate constants and 36 species participating in the reaction. At the instant corresponding to the calculated value $\tau_{ind, AMP} = 4$ min, the relative specific rate of AMP formation (r_{AMP}) is determined by the monomer $Op(OH^-)_2$ concentration to a degree of 97.9%. The concentrations of trimeric species $(DOH^-)H^+ \cdot$ Cy and $(DOH^-)H^+ \cdot$ Op contribute 1.9%, and the concentration of dimers $(DOH^-)H^+$ contributes 0.2%.

$$r_{AMP} = [(DOH^-)H^+] \times 1 + \{[(DOH^-)H^+ \cdot Cy] + (DOH^-)H^+ \cdot Op]\} \times 3 + [Op(OH^-)_2] \times 4.5.$$

Coefficients 1, 3, and 4.5 are the ratios of rate constants of steps 15, 15', and 8. The dependence of dimer concentration on time passes through a maximum at $t \approx 62$ min. At this time, the relative specific rate of ADP formation (r_{ADP}) is determined by the monomer $CyOH^-$ concentration to a degree of 93.2%. The concentrations of trimeric species T1 and T2 contribute 2.4%, and the concentration of D contributes 4.4%.

$$r_{ADP} = [D] \times 0.9 + ([T1] + [T2]) \times 2.2 + [CyOH^-] \times 0.7.$$

The coefficients reflect the ratio of the rate constants of step 2 (k_2), 2' ($k_{2'}$), and 1 (k_1). Figure 11 shows the results of analogous calculations for run 6 (pH 9.02). When the dimer concentration is maximal, r_{ADP} is determined by the $CyOH^-$ concentration to a degree of 97%. The relative specific rate of AMP formation at the end of the induction period is determined by the $Op(OH^-)_2$ concentration to a degree of 99.3%.

Because the rate of hydrolysis at high pH basically depends on the concentrations of monomeric species, which change substantially at early reaction stages due to the fast formation of intermediate products (Op'OH^-,

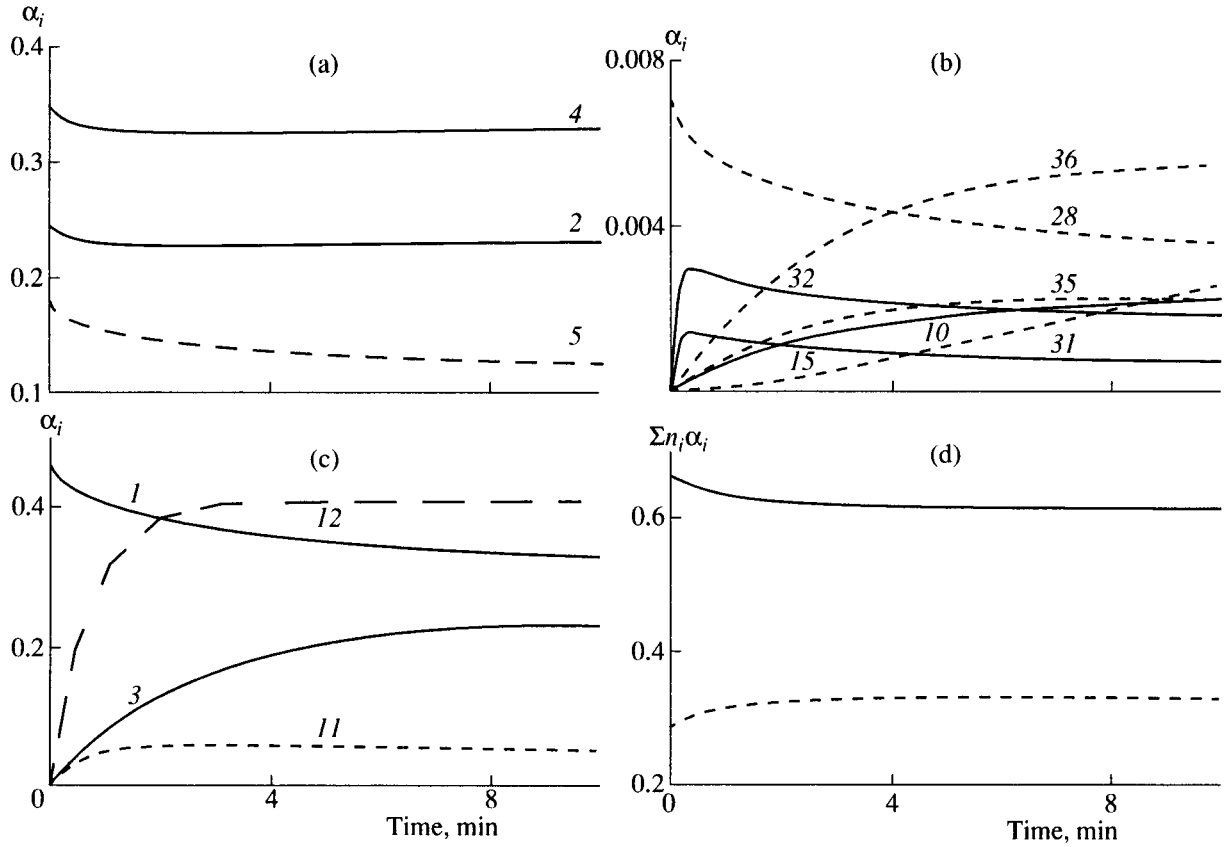

Fig. 12. Variation in (a–c) the concentration of intermediate products and (d) the overall concentration of ions and $ZnATP^{2-}$ molecules during hydrolysis at pH 8.50 and 50°C (run 1, Table 1) at an early stage of hydrolysis: (*1*) $CyOH^-$, (*2*) $OpOH^-$, (*3*) $Op(OH^-)_2$, (*4*) Op, (*5*) Cy, (*11*) $Cy'OH^-$, (*12*) $Op'OH^-$, (*15*) $(DOH^-)H^+$, (*35*) $(DOH^-)H^+ \cdot$ Cy, and (*36*) $(DOH^-)H^+ \cdot$ Op. The dashed line in figure (d) is the overall concentration of ions. The solid line is the overall concentration of $ZnATP^{2-}$ molecules. The calculation was performed by Scheme 3.

$Cy'OH^-$, and $Op(OH^-)_2$, then a reasonable question arises as to how this is reflected in the initial concentrations of intermediate products calculated from the pH-dependent equilibrium distribution of the concentrations of species that are present in the aqueous solution of Zn · ATP (1:1) [6]. According to the data of [6], $ZnATP^{2-}$, $ZnATP^{2-}OH^-$, and 4–6 mol % of ATP^{4-} not bound to a Zn^{2+} complex are in equilibrium at pH 7–9. As pH increases, the fraction of $ZnATP^{2-}$ decreases, and the fraction of $ZnATP^{2-}OH^-$ increases because of the deprotonation of the water molecule coordinated to Zn^{2+} in $ZnATP^{2-}$ complexes. Let us analyze the effect of fast steps of intermediate product formation on a change in the sum of the ion concentrations and the concentrations of $ZnATP^{2-}$ molecules. Figure 10 (c and d) shows that the main change in these overall concentrations at pH 8.84 takes place during the first 2 min after the reaction start; then, this change is small. The sum of ion concentrations is $[CyOH^-] + [OpOH^-] + [Op(OH^-)_2] + [Op'OH^-] + [Cy'OH^-]$. The sum of the first two terms decreases and the sum of the other terms increases. The overall sum increases. The sum of the concentrations of $ZnATP^{2-}$ molecules is $[Op] + [Cy] + [Op'] + [Op''] + 2[K(ATP)] + 3[K_{(T1)}] + 3[K_{(T2)}] + 2[D] + 2[(DOH^-)H^+] + 3([(DOH^-)H^+ \cdot Cy] + [(DOH^-)H^+ \cdot Op]) + 3([T1] + [T2])$. During the process, the sum of the first seven terms decreases, and the sum of the next three terms increases. The value of the last term has a maximum at ~0.26 min. The overall sum decreases. Two minutes after the start of the reaction, the overall concentration of ions at pH 8.84 increases by 12% compared to the initial value, and the overall concentration $[ZnATP^{2-}]$ decreases by 12%. At pH 9.02, an overall increase in the number of ATP molecules in the ions is 12%, and the overall change $\Sigma[ZnATP^{2-}]$ is 18% compared to the initial value. Figure 12 shows the concentration profiles for the intermediate products at an early stage of hydrolysis at pH 8.50. Under these conditions, the overall change in the number of $ZnATP^{2-}$ molecules includes some contribution of the associates K(ATP), T1, T2, $(DOH^-)H^+ \cdot$ Cy, and $(DOH^-)H^+ \cdot$ Op. Two minutes after the start of the reaction, the $\Sigma[ZnATP^{2-}]$ changes by 5.5%, and the overall concentration of ion changes by 12% compared to the initial values. At pH 8.73, these changes for 2 min are 9.7 and 12.4%, respectively. These data refer to hydrolysis at 50°C. The results of potentiometric titration were obtained at 25°C. Therefore, we expect that the overall initial concentrations of ions and $ZnATP^{2-}$ molecules will change until $t \approx 4$–6 min, which is a period during

which the curve of potentiometric titration is obtained during the stepwise addition of NaOH and pH settling. Probably, when we use potentiometric titration data for $[ZnATP^{2-}]_0$ calculation, we somewhat underestimate the overall concentration of $ZnATP^{2-}$ molecules. The higher pH, the more pronounced this effect.

The results of the mathematical analysis of hydrolysis kinetics at high pH completely agrees with the main idea underlying the model of the active dimer complex: in the active center, M^{2+} should be bound only to the γ-phosphate group, whereas the open species (supposedly, β,γ-complexes Op and $OpOH^-$) are inactive in the selective ADP formation. Their transformation to active γ-complexes occurs via several consecutive steps of isomeric transformation, which limits the overall rate of hydrolysis at pH ≥ 8.5. Our ideas emphasize the relationships between the conformation of the $MATP^{2-}$ complex and the selectivity to hydrolysis products. We propose a new pathway for the formation of the attacking nucleophile and defend the idea of the solvation of the proton that participates in the formation of a strong hydrogen bond during the formation of intermediate complexes. This mechanism dominates in a hydrophobic environment, because it allows the solvation of a proton from a coordinated water molecule in the absence of the aqueous medium. Note that for the catalytic centers of ATP-ases the hydrophobic environment is typical [45]. It follows from the schemes proposed for isomeric transformation (Schemes 1a and 2a) that the abstraction of OH^- from the γ-P atom of the pentacovalent intermediate after pseudotransformation occurs in both binary ($MATP^{2-}$) and ternary mixed-ligand ($MATP^{2-}OH^-$) complexes where OH^- is the third ligand. We believe that a change in the ATP-ase conformation occurs at the stages of formation and decomposition of hydrolysis pentacovalent intermediates, which are formed by the addition of H_2O or OH^- to γ-P.

ACKNOWLEDGMENTS

This work was supported by grant no. JII100 from the International Science Foundation and Russian government and grant no. 96-03-32649 from the Russian Foundation for Basic Research.

APPENDIX

Let us consider an example of choosing the initial conditions in the calculations of concentration profiles during hydrolysis at pH 8.73 (see Table 7 for run 3 from Table 1).

The initial concentration $[NuP]_0 = 2.83 \times 10^{-3}$ mol/l is the overall concentration of nucleoside-5'-phosphates in the reaction mixture before the start of the

Table 7

No.	Intermediate product	Initial concentration (Scheme 2)	Initial concentration (Scheme 3)	No.	Intermediate product	Initial concentration (Scheme 2)	Initial concentration (Scheme 3)
1	$CyOH^-$	0.061	0.063	19*	$ZnATP^{2-}$	1.49×10^{-3}	1.49×10^{-3}
2	$OpOH^-$	0.320	0.320	20	K(ADP)	3.26×10^{-6}	3.36×10^{-6}
3	$Op(OH^-)_2$	0	0	21	Cy(ADP)	1.69×10^{-3}	1.69×10^{-3}
4	Op	0.269	0.278	22	Op(ADP)	8.3×10^{-4}	8.3×10^{-4}
5	Cy	0.136	0.141	23	$OpOH^-$(ADP)	5.68×10^{-3}	5.68×10^{-3}
6	ADP	0.014	0.014	24	$CyOH^-$(ADP)	5.80×10^{-3}	5.80×10^{-3}
7	AMP	0.0139	0.0139	25	$Op(OH^-)_2$(ADP)	0	0
8*	OH^-	2.94×10^{-5}	2.94×10^{-5}	26	HPO_4^-	0.0136	0.0136
9*	H^+	1.86×10^{-9}	1.86×10^{-9}	27	D(ADP)	2.1×10^{-6}	1.4×10^{-6}
10	D	0.0136	0	28	K(ATP)	–	4.52×10^{-3}
11	$Cy'OH^-$	0	0	29	K(T1)	–	0
12	$Op'OH^-$	0	0	30	K(T2)	–	0
13	Op'	0.047	0.049	31	T1	–	0
14	Op"	0.047	0.049	32	T2	–	0
15	$(DOH^-)H^+$	0	0	33	T1'	–	0
16*	NuP_0	2.83×10^{-3}	2.83×10^{-3}	34	T2'	–	0
17	$H_2PO_4^-$	0.0004	0.0004	35	$(DOH^-)H^+ \cdot Cy$	–	0
18	D'	0	0	36	$(DOH^-)H^+ \cdot Op$	–	0

Note: The concentrations of all intermediate products are in molar fractions of $[NuP]_0$ excluding those marked with an asterisk. The concentrations of products 8, 9, 16, and 19 are in mol/l.

reaction determined by spectrophotometry. $[Zn \cdot ATP]_0 = 2.71 \times 10^{-3}$ mol/l; $[ZnATP^{2-}] = a \times 2.71 \times 10^{-3}$ mol/l. According to [6], 0.55 parts of $ZnATP^{2-}$ species (a), 0.049 parts of ATP^{4-} not bound to Zn^{2+}, and 0.401 parts of $ZnATP^{2-}OH^-$ are in equilibrium at pH 8.73. Scheme 2 assumes that $[Op]_0 + [Op']_0 + [Op'']_0)/[Cy]_0 = 2.66$; $[ZnATP^{2-}]_0 = [Cy]_0 + [Op]_0 + [Op']_0 + [Op'']_0 + 2[D]_0$; and $[NuP_0] = [CyOH^-]_0 + [OpOH^-]_0 + [Cy]_0 + [Op]_0 + [Op']_0 + [Op'']_0 + 2[D]_0 + [ATP^{4-}]_0 + [ADP]_0 + [AMP]_0$. The concentrations $[CyOH^-]_0$ and $[OpOH^-]_0$ listed below were calculated from $K_{a,Cy}$ and $K_{a,Op}$ (see text). The $[ATP^{4-}]/[NuP]_0$ ratio takes into account the concentration of ATP^{4-}, which is in equilibrium with $ZnATP^{2-}$ and $ZnATP^{2-}OH^-$ (4.7 mol % in portions of $[NuP]_0$) and the concentration of excess ATP^{4-} (1.4 mol %). The sum $[CyOH^-]_0 + [OpOH^-]_0$ calculated from the adopted K, $K_{a,Cy}$ and $K_{a,Op}$ values is 1.08×10^{-3} mol/l. The overall concentration $[ZnATP^{2-}OH^-]_0$ in the balance of $[Zn \cdot ATP]_0$ is 1.09×10^{-3} mol/l according to the potentiometric data. The imbalance in $[NuP]_0$ is 0.5%. In the series of runs at 8.5–9.0, the imbalance is 0.2–1.0%. The maximal imbalance (3.5%) was observed at pH 8.5. That is, the values of $K_{a,Cy}$ and $K_{a,Op}$ used in the calculation adequately describe the dependence of $\Sigma[CyOH^-]_0 + [OpOH^-]_0$ on pH.

According to Scheme 3 $[Op]_0 + [Op']_0 + [Op'']_0)/[Cy]_0 = 2.66$, $[ZnATP^{2-}]_0 = [Cy]_0 + [Op]_0 + [Op']_0 + [Op'']_0 + 2[K(ATP)]_0$; the contributions of $[K_{T1}]_0$ and $[K_{T2}]_0$ are much smaller than that of $[K(ATP)]_0$; and $[NuP_0] = [CyOH^-]_0 + [OpOH^-]_0 + [Cy]_0 + [Op]_0 + [Op']_0 + [Op'']_0 + 2[K(ATP)]_0 + [ATP^{4-}]_0 + [ADP]_0 + [AMP]_0$. The sum $[CyOH^-]_0 + [OpOH^-]_0$ calculated using the above values of $K_{a,Cy}$, and $K_{a,Op}$ is 1.11×10^{-3} mol/l. The deviation of the overall concentration $[ZnATP^{2-}OH^-]_0$ is 0.7% in the balance of $[NuP]_0$. In the series of runs at pH 8.5–9.0, this deviation is 0.7–3.0%.

In the aqueous solution, ADP is a mixture of several species which are in fast equilibrium. Therefore, the calculated fraction of ADP in the balance of $[NuP]_0$ is the sum $[ADP] = [D'] + [K(ADP)] + [Cy(ADP)] + [Op(ADP)] + [CyOH^-(ADP)] + [OpOH^-(ADP)] + [Op(OH^-)_2(ADP^-)] + 2[D(ADP)]$ at any moment of time. At zero time, the initial concentration of ADP is $[Cy(ADP)] + [Op(ADP)] + [CyOH^-(ADP)] + [OpOH^-(ADP)]$. The concentrations of ions are higher than the concentration of $ZnADP^-$ complexes, although all these values are small. Under the conditions considered here, the formation of ADP is irreversible.

REFERENCES

1. Sigel, H., Hofstetter, F., Martin, R.B., *et al., J. Am. Chem. Soc.*, 1984, vol. 106, no. 25, p. 7935.
2. Kochetkov, S.P., Gabibov, A.G., and Severin, E.S., *Bioorg. Khim.*, 1984, vol. 10, no. 10, p. 1301.
3. Mildvan, A.S., *Annu. Rev. Biochem.*, 1974, vol. 43, p. 357.
4. Sigel, H., *Metal–DNA Chemistry*, Tullius, T.D., Ed., Washington: American Chemical Society, 1989, p. 159.
5. Sigel, H., *Coord. Chem.*, 1990, vol. 100, p. 453.
6. Amsler, P. and Sigel, H., *Eur. J. Biochem.*, 1976, vol. 63, no. 3, p. 569.
7. Creaser, I.I., Haightt, G.P., Peachey, R., *et al., J. Chem. Soc., Chem. Commun.*, 1984, p. 1568.
8. Sigel, H. and Tribolet, R., *J. Inorg. Biochem.*, 1990, vol. 40, no. 2, p. 163.
9. Norman, P.R., Giletti, P.F., and Cornelius, R.D., *Inorg. Chim. Acta,* 1984, vol. 82, no. 1, p. L5.
10. Haight, G.P., *Coord. Chem. Rev.*, 1987, vol. 79, no. 3, p. 293.
11. Norman, P.R. and Cornelius, R.D., *J. Am. Chem. Soc.*, 1982, vol. 104, no. 9, p. 2356.
12. Cornelius, R.D. and Norman, P.R., *Inorg. Chim. Acta,* 1982, vol. 65, no. 5, p. L193.
13. Blackburrn, G.M., Thatcher, G.R.J., Hosseini, M.W., *et al., Tetrahedron Lett.*, 1987, vol. 28, no. 24, p. 2779.
14. Hosseini, M.W., Lehn, J.-M., Maggiora, L., *et al., J. Am. Chem. Soc.*, 1987, vol. 109, no. 2, p. 537.
15. Hubner, P.W.A. and Milburn, R.M., *Inorg. Chem.*, 1980, vol. 19, no. 5, p. 1267.
16. Yohannes, P.G., Plute, K.E., Mertes, M.P., *et al., Inorg. Chem.*, 1987, vol. 26, no. 11, p. 1751.
17. Meyer, G.R. and Cornelius, R.D., *J. Inorg. Biochem.*, 1984, vol. 22, no. 4, p. 249.
18. Ramirez, F., Marecek, J.F., and Scamosi, J.J., *J. Org. Chem.*, 1980, vol. 45, no. 23, p. 4748.
19. Hediger, M. and Milburn, R.M., *J. Inorg. Biochem.*, 1982, vol. 16, no. 2, p. 165.
20. Massoud, S.S. and Milburn, R.M., *J. Inorg. Biochem.*, 1990, vol. 39, no. 4, p. 337.
21. Tafesse, F., Massoud, S.S., and Milburn, R.M., *Inorg. Chem.*, 1985, vol. 24, no. 17, p. 2591.
22. Tafesse, F., Massoud, S.S., and Milburn, R.M., *Inorg. Chem.*, 1993, vol. 32, no. 9, p. 1864.
23. Massoud, S.S., *J. Inorg. Biochem.*, 1994, vol. 55, no. 3, p. 183.
24. Wolcott, R.G. and Boyer, P.D., *Biochem. Biophys. Res. Commun.*, 1974, vol. 57, no. 3, p. 709.
25. Syrtsova, L.A., *Usp. Biol. Khim.*, 1989, vol. 30, p. 130.
26. Kandpal, R.P., Stempel, K.E., and Boyer, P.D., *Biochemistry*, 1987, vol. 26, no. 6, p. 1512.
27. Sigel, H., *Eur. J. Biochem.*, 1987, vol. 165, no. 1, p. 65.
28. Sigel, H., Tribolet, R., Malini-Balakrishnan, R., *et al., Inorg. Chem.*, 1987, vol. 26, no. 13, p. 2149.
29. Sigel, H., Scheller, K.H., and Milburn, R.M., *Inorg. Chem.*, 1984, vol. 23, no. 13, p. 1933.
30. Tribolet, R., Martin, R.B., and Sigel, H., *Inorg. Chem.*, 1987, vol. 26, no. 5, p. 638.
31. Scheller, K.H., Hofstetter, F., Mitchell, P.R., *et al., J. Am. Chem. Soc.*, 1981, vol. 103, no. 2, p. 247.
32. Wang, X., Nelson, D.J., Trindle, C., *et al., J. Inorg. Biochem.*, 1997, vol. 68, no. 1, p. 7.
33. Sigel, R.K.O., Song, B., and Sigel, H., *J. Am. Chem. Soc.*, 1997, vol. 119, no. 4, p. 744.
34. Ramirez, F. and Marecek, J.F., *Biochim. Biophys. Acta*, 1980, vol. 589, no. 1, p. 21.

35. Huang, S.L. and Tsai, M.D., *Biochemistry*, 1982, vol. 21, no. 5, p. 951.
36. Matthies, M. and Zundel, G., *J. Chem. Soc., Perkin Trans. II*, 1977, p. 1824.
37. Takeuchi, H., Murata, H., and Harada, I., *J. Am. Chem. Soc.*, 1988, vol. 110, no. 2, p. 392.
38. Utyanskaya, E.Z. and Shilov, A.E., *Kinet. Katal.*, 1988, vol. 29, no. 1, p. 136.
39. Utyanskaya, E.Z., Pavlovskii, A.G., Sosfenov, N.I., *et al.*, *Dokl. Akad Nauk SSSR*, 1988, vol. 301, no. 1, p. 149.
40. Utyanskaya, E.Z., Pavlovskii, A.G., Sosfenov, N.I., *et al.*, *Kinet. Katal.*, 1989, vol. 30, no. 6, p. 1343.
41. Utyanskaya, E.Z., Pavlov, A.O., Orekhova, E.M., *et al.*, *Kinet. Katal.*, 1991, vol. 32, no. 2, p. 349.
42. Utyanskaya, E.Z., Neihaus, M.G., Lidskii, B.V., *et al.*, *React. Kinet. Catal. Lett.*, 1995, vol. 54, no. 2, p. 431.
43. Utyanskaya, E.Z., Mikhailova, T.V., Pavlov, A.O., *et al.*, *ACH-Models in Chemistry*, 1996, vol. 133, nos. 1–2, p. 65.
44. Utyanskaya, E.Z., Shilov, A.E., Lidskii, B.V., *et al.*, *ACH-Models in Chemistry*, 1996, vol. 133, no. 4, p. 365.
45. de Meis, L., Behrens, M.I., Celis, H., *et al.*, *Eur. J. Biochem.*, 1986, vol. 158, no. 1, p. 149.
46. Ceck, T.R., *Science*, 1987, vol. 236, no. 4808, p. 1532.
47. Pan, T. and Uhlenbeck, O.C., *Nature*, 1992, vol. 358, no. 6387, p. 560.
48. Utyanskaya, E.Z., Pavlov, A.O., Orekhova, E.M., *et al.*, *Zh. Anal. Khim.*, 1990, vol. 45, no. 6, p. 1222.
49. Bell, R.P., *The Proton in Chemistry*, London: Chapman and Hall, 1973, p. 355.
50. Westheimer, F.H., *Rearrangements in Ground and Excited States*, de Mayo, R., Ed., New York: Academic, 1980, p. 229.
51. Anslyn, E. and Breslow, R., *J. Am. Chem. Soc.*, 1989, vol. 111, no. 12, p. 4473.
52. Breslow, R. and Huang, D.-L., *Proc. Natl. Acad. Sci. U.S.A.*, 1991, vol. 88, no. 10, p. 4080.